Applied Catalysis B: Environmental 98 (2010) 10–26

Contents lists available at ScienceDirect

Applied Catalysis B: Environmental

journal homepage: www.elsevier.com/locate/apcatb

Review

# Heterogeneous photo-Fenton oxidation with pillared clay-based catalysts for wastewater treatment: A review

J. Herney-Ramirez [a], Miguel A. Vicente [b], Luis M. Madeira [c,*]

[a] Universidad Nacional de Colombia, Facultad de Ingeniería, Departamento de Ingeniería Química y Ambiental, Carrera 30 Nº 45-03, Bogotá, DC, Colombia
[b] Departamento de Química Inorgánica, Universidad de Salamanca, Plaza de la Merced, S/N E-37008 Salamanca, Spain
[c] LEPAE, Department of Chemical Engineering, Faculty of Engineering – Porto University, Rua Dr. Roberto Frias, 4200-465 Porto, Portugal

ARTICLE INFO

*Article history:*
Received 23 February 2010
Received in revised form 28 April 2010
Accepted 1 May 2010
Available online 11 May 2010

*Keywords:*
Pillared clays
Heterogeneous catalyst
Photo-Fenton
Wastewater treatment
Advanced Oxidation Processes

ABSTRACT

Due to their excellent properties, pillared clays (PILCs) have been widely used in several applications, particularly in catalysis. In this paper, their use in heterogeneous photo-Fenton-like advanced oxidation for wastewater treatment, employing either model/synthetic effluents or real streams, is reviewed. Particular attention is given to the effect that the main operating conditions have on process performance, namely wavelength of the light source and power, initial $H_2O_2$ or parent compound concentration, catalyst load, pH and temperature. Emphasis is also given to the type of catalyst used and its synthesis conditions (e.g. thermal aging or acid treatment). Several important technological aspects that should be accounted for in real practice are also discussed in detail, particularly the catalyst stability, the use of continuous-flow fixed-bed reactors, the mode of oxidant addition, the environmental impact/integration with biological processes and the possibility of using visible light instead of UV only. Then, some simple mechanistic studies reported are summarized, as well as modeling works.



**Contents**



* Corresponding author. Tel.: +351 22 5081519; fax: +351 22 5081449.
*E-mail address:* mmadeira@fe.up.pt (L.M. Madeira).

0926-3373/$ – see front matter © 2010 Elsevier B.V. All rights reserved.
doi:10.1016/j.apcatb.2010.05.004

## 1. Introduction

### 1.1. Fundamentals on the photo-Fenton and other Advanced Oxidation Processes (AOPs)

Water is used in agriculture, construction, transport, chemical industry, and in numerous other activities of the human beings. According to the United Nations, the first priority of poor countries, especially in Africa, should be not financial support or technological knowledge but clean water supply to the population [1].

The typical processes used to decontaminate wastewaters are physical, biological and chemical. All these treatments can be used separately or combined with other processes to enhance the overall treatment efficiency. The choice of the correct system must be carried out considering several factors, both technical (treatment efficiency, plant simplicity, etc.) and economical (investment and operating costs). However, the typical treatment methods present some disadvantages, which include the following: (i) high cost (e.g. incineration), (ii) an apparent low cost option is offered by the biological oxidation, but the organic pollutant/s has/have to be biodegradable, diluted and of low toxicity, and (iii) transfer of the aqueous organics to another phase, leaving the contaminants undestroyed (adsorption). Summarizing, the actual conventional methods are clearly not suitable to treat toxic, non-biodegradable organic pollutants, and new improved treatment methods have to be developed and tested.

To overcome the inconveniences of conventional treatment methods, various chemical oxidation techniques have emerged in the last decades, in particular for the treatment of industrial wastewaters. Among these techniques, the so-called advanced oxidation processes appear to be a promising field of study, which have been reported to be effective for the degradation of soluble organic contaminants in waters and soils. Actually, they can often provide an almost total degradation, under reasonably mild conditions of temperature and pressure [2–4]. These processes are particularly characterized by the deep changes that they produce in the chemical structure of the contaminants present in waters/wastewaters.

AOPs not only transform chemically polluting agents, but present very attractive advantages, such as the complete mineralization of some compounds, their oxidation at very low concentrations, the generation of environmentally friendly by-products, the improvement in the organoleptic properties of the treated water and the low consumption of energy, in comparison with other methods. These processes utilize chemical reactions, electron beams, UV light or ultrasound pulses, for instance, to obtain high oxidation rates through the generation of free radicals (mainly hydroxyl radicals). Indeed, highly reactive hydroxyl radicals ($HO^{\bullet}$) are traditionally thought to be the main active species responsible for the destruction of the pollutants [5–7].

Many AOPs use hydrogen peroxide as the main oxidizing agent, which is a reagent more efficient than gaseous oxygen concerning the contaminants mineralization, allowing also the diminution of the residence times in the oxidation process, especially when focusing dangerous polluting compounds [8]. Besides, $H_2O_2$ is not of environmental concern and its self decomposition yields water and oxygen. Among the processes using this oxidant, the photo-Fenton is worth of noting. Although photo-Fenton has been much studied in the last years (e.g. [9–12]), the homogeneous photo-Fenton process requires complementary steps, such as precipitation, to recover the iron catalyst, prevent contamination and enable catalyst re-use. This way, the cost of the homogeneous processes depends largely on the supply of chemicals, power and labour requirements. Because of these disadvantages, several attempts have been made to develop solid supports for the active iron species. Hopefully, these materials should exhibit high catalytic activity in the photo-Fenton processes, but should be also stable, not loosing the metal by leaching [13–15]. Using more or less simple techniques, metal oxides may be included in different solid supports, such as clays [11]. The use of this kind of heterogeneous catalysts is particularly beneficial because very often complete mineralization of the organic pollutant can be reached, along with easy separation of the catalysts from the treated wastewater, not causing secondary metal ion pollution. In addition to these advantages, the wide use of pillared clay-based catalysts (PILCs) as catalyst support is due to the fact that natural clays are cheap, abundant and the process of preparation is very simple. PILCs are attractive as adsorbents, catalysts or catalyst support also due to their high specific surface areas [16–18]. The main characteristics of the clay-based catalysts most used in photo-Fenton reactions will be very briefly summarized in the next section.

The Fenton's process has its origin in the discovery reported in 1894 that ferrous ion strongly promotes the oxidation of tartaric acid by hydrogen peroxide [19]. However, only much later the oxidation activity has been ascribed to the hydroxyl radical [20]. The mechanism of the Fenton's process is quite complex, and some papers can be found in the literature where tens of equations are used for its description [21,22]. Nevertheless, it can be summarized by the following steps: first, a mixture of $H_2O_2$ and ferrous iron in acidic solution generates the hydroxyl radicals (Eq. (1)) [23–26], which will subsequently attack the organic compounds present in the solution.

$$Fe^{2+} + H_2O_2 \rightarrow Fe^{3+} + HO^- + HO^{\bullet} \quad (1)$$

As iron(II) acts as a catalyst, it has to be regenerated, which seems to occur through the following scheme:

$$Fe^{3+} + H_2O_2 \leftrightarrow Fe\text{–}OOH^{2+} + H^+ \quad (2)$$

$$Fe\text{–}OOH^{2+} \rightarrow Fe^{2+} + HO_2^{\bullet} \quad (3)$$

Oxidation with the Fenton's reagent has already proved to be effective and promising for the destruction of several compounds, and consequently for the treatment of a wide range of wastewaters, as described in several reviews (e.g., [2,22,27,28]).

The photo-Fenton process, as its name suggests, is rather similar to the Fenton one, but employing also radiation [22,29,30]. Its effectiveness is attributed to the photolysis of Fe(III) cations in acidic media yielding Fe(II) cations (Eq. (4)), in conjunction with reaction between Fe(II) and $H_2O_2$ to yield hydroxyl radicals (Fenton's

reaction, step (5)):

$$Fe(OH)^{2+} + h\nu \rightarrow Fe^{2+} + HO^{\bullet} \quad (4)$$

$$Fe^{2+} + H_2O_2 \rightarrow Fe(OH)^{2+} + HO^{\bullet} \quad (5)$$

In this process, the regeneration of $Fe^{2+}$ by photo-reduction of $Fe^{3+}$ (Eq. (4)) is accelerated, this photo-reduction being an additional source of highly oxidative hydroxyl radicals, as compared with the "simple" Fenton's process. Actually, in the latter, the overall rate of regeneration and process efficiency are considerably low, as discussed elsewhere [28]. Nevertheless, the importance of the regeneration of $Fe^{2+}$ through another step, namely the photo-reduction of the photochemical organic substrate or its degradation intermediates has been pointed out by some authors [31]:

$$Fe^{3+}L + h\nu \rightarrow Fe^{2+} + L^{\bullet} \quad (L = RCOO^{-},\ RO^{-},\ HO^{-}) \quad (6)$$

Besides Fe, other transition metals can catalyze also the reactions mentioned above, e.g. copper. In fact, the reaction system using Cu as the photo-Fenton catalyst follows a similar network as that of Fe and is referred to as a photo-Fenton-like reaction [32].

Recently, much attention has been paid to the photo-Fenton and photo-Fenton-like processes, mainly focusing on the heterogeneous process [31]. This is much related to the disadvantages associated to the homogeneous process, namely the formation at the end of the process of high amounts of metal-containing sludges, with high environmental impact and costs associated. In addition, large amount of the catalytic metals are lost in these sludges. In the opinion of some authors, the costs associated with the processing of these sludges might limit the further application of the homogeneous photo-Fenton process [e.g. 32,33], reason by which numerous attempts have been done to find heterogeneous systems/supports for the Fe species, as pillared clays, for subsequent use in photo-Fenton-based processes.

### 1.2. Fundamentals on clay-based catalysts used in photo-Fenton processes

As indicated, the photo-Fenton reaction has been widely applied under homogeneous conditions, being an effective method for the removal of a high variety of contaminants, with the important advantages of working under simple operation conditions and the low price of the oxidation reagents. However, this application has various serious disadvantages, as discussed above, namely the formation of Fe-containing sludges. On the other hand, the effectiveness of the catalysts is sometimes decreased by different effects, the most important is the presence in the wastewater, as original contaminants or as intermediate compounds, of ligands with high preference by $Fe^{2+/3+}$ cations, such as oxalate anions, which may irreversible coordinate iron. All these problems strongly suggest the use of heterogeneous catalysis as alternative for this reaction.

Obviously, very different iron-containing catalysts can be used for this process. First, bulk catalysts containing this element may be considered, as hematite, goethite or magnetite. A different approach is the incorporation of iron into different supports, being zeolites, polymers or carbon proposed by different authors, but clays also appearing as an interesting alternative [34–38].

The incorporation of iron into clays can be done by different strategies. The simplest one may be the cationic exchange of the exchangeable cations of the clay, but this may lead to contents of iron too low. Thus, pillaring and impregnation appear as more effective methods.

$Fe^{3+}$ can polymerize, forming polycationic species. Unfortunately, this polymerization is very difficult to be reproduced, as very small changes in the conditions strongly affect the process, and iron hydroxides are very easily formed. Besides, the structure of the polymers is not well established, and their stability is low. In spite of this, several examples of smectite clays pillared with iron polycations are reported in the literature. Having in mind the well-known structure, synthesis conditions, stability, etc. of $[Al_{13}O_4(OH)_{24}(H_2O)_{12}]^{7+}$ polycation, usually known as $Al_{13}$ Keggin polycation, co-polymerization of $Al^{3+}$ and $Fe^{3+}$ appears as an attractive method for incorporation of iron. This has been studied by several authors, and effective incorporation of iron (in some cases, also doping with Cu) has been reported [39]. There is however a strong controversy in the literature about the nature of the polycations formed from solutions containing $Al^{3+}$ and $Fe^{3+}$. Actually, several authors have reported that both elements polymerize separately while other authors think that $Fe^{3+}$ can effectively substitute isomorphically $Al^{3+}$ in the structure of $Al_{13}$ Keggin polycation [39–52]. In any case, the important result is that iron is incorporated into the solids and that the catalytic behavior of the solids is thus enhanced. Besides, it has been reported that Fe-species associated to the pillars are catalytically more effective and more resistant to leaching than other Fe-species [53].

However, an important disadvantage of co-polymerization of $Al^{3+}$ and $Fe^{3+}$ is that it is not possible to control the amount of iron incorporated to the clay. Thus, an alternative strategy is to pillar first the clay with $Al_{13}$ Keggin polycation, and to use the very stable Al-PILC thus obtained as support to be impregnated with Fe-precursors in a subsequent step. Several examples of clay-based impregnated catalysts with predetermined contents of iron are thus reported in the literature. As in the case of the pillared clays, the impregnated solids must be calcined before their use as catalysts, and although the active species are expected to be similar in both processes (iron oxy-hydroxides), it may also be expected that they may have different properties (particle size, dispersion degree, location in the structure of the solids). In any case, solids prepared both by co-pillaring of Al and Fe and by impregnation have proved to be effective catalysts in photo-Fenton processes, as may be reviewed in this article.

### 1.3. Pollutants degraded or wastewaters treated with pillared clay-based catalysts

As mentioned, PILCs have been extensively used in photo-Fenton-like processes. Table 1 provides an overview of the model pollutants degraded by such processes, as well as of the real effluents treated, the PILC catalysts used, the best (or typical) performances reached, as well as the corresponding operating conditions. Without aiming to go into much detail in the analysis of each work, it is important to do an overall appreciation, so that the reader might become aware of the conditions employed and performances reached. Obviously this depends on the particular application envisaged, but in general temperatures are close to 25–30 °C, initial pH to about 3 and operation has most often been done in batch reactors with catalyst doses of around 1 g/L. The light source has usually been of the UV-C type (254 nm) and the conversions reached depend clearly on the conditions applied, reaction time and wastewater to be treated.

Several substances are referred therein, being of particular relevance phenols (and their derivatives). The reasons for the significant amount of papers related to such compounds are simple: phenols are used in many industries, and thus are present in the corresponding waste streams. In particular, phenol world production is estimated to be over $3 \times 10^6$ tons/year [54], being used in the synthesis of many substances (e.g., resins, dyes, pharmaceuticals, perfumes, pesticides, tanning agents, solvents or lubricating oils). Besides, it has several concerns to human health, its biodegradability is low and is toxic [54].

Tyrosol (*p*-hydroxyphenylethanol) has also deserved the attention of some researchers because it is a representative compound of the polyphenolic fraction typically found in olive processing

**Table 1**
Some examples of degradation of organic substances, or real effluents, using photo-Fenton and photo-Fenton-like AOPs catalyzed by pillared clays.

| Clay catalyst | Catalytic test | | Best (or typical) performances reached | Reference |
|---|---|---|---|---|
| | Organic pollutant | Operating conditions | | |
| Fe-laponite | Phenol | $T$ = 30 °C; UV-C (254 nm); pH 3; 1 $g_{catalyst}$/L; 50 mM $H_2O_2$; 1 mM phenol; $H_2O_2$/Ph = 50 (molar ratio) | $X_{phenol} \sim 100\%$ ($t$ = 5 min) | [54] |
| AlFe-montmorillonite | Phenol | 5 mg phenol/L; pH 3.5–4.0; 5 $g_{cat}$/L; 2 mM $H_2O_2$; Air flow = 30–35 $cm^3$/min; Room temperature; Halogen lamp (CE 220/240 V/50 Hz-50 W); $H_2O_2$/Ph = 37.6 (molar ratio) | $X_{phenol}$ = 100% ($t$ = 1 h) | [55] |
| AlFe-montmorillonite | Tyrosol | [Tyrosol] = 500 ppm; initial pH 3; $T$ = 25 °C; 20 mM $H_2O_2$; 30 W UV-lamp ($\lambda$ = 254 nm); 0.5 $g_{cat}$/L; $H_2O_2$/tyrosol = 5.5 (molar ratio) | $X_{tyrosol}$ = 100%; $X_{TOC}$ = 50% ($t$ = 24 h) | [56] |
| AlFe-montmorillonite | Model OMW (8 low-molecular mass phenolic compounds present in olive mill wastewater—OMW) | $C_o$ (total phenol) = 0.5 g/L; Initial pH 5; $T$ = 25 °C; 20 mM $H_2O_2$; 30 W UV-lamp ($\lambda$ = 254 nm); 0.5 $g_{cat}$/L | $X_{caffeic\ acid}$ = 86%; $X_{hydroxytyrosol}$ = 70% ($t$ = 24 h) | [57] |
| AlFe-montmorillonite | Real OMW (obtained by ultrafiltration of crude OMW) | 20 mM $H_2O_2$; 30 W UV-lamp ($\lambda$ = 254 nm); 0.5 $g_{cat}$/L | $X_{total\ phenols}$ = 62%; $X_{TOC}$ = 43% ($t$ = 24 h) | [57] |
| CuAl-montmorillonite | Real OMW | 2.2% $H_2O_2$ (v/v); UV-lamp (366 nm); 0.5 $g_{cat}$/L | $X_{TOC}$ = 45% ($t$ = 2 h) | [58] |
| Fe-laponite | Azo-dye acid black 1 (AB1) | 6.4 mM $H_2O_2$; 1.0 g Fe-Lap-RD/L; 8 W UVC (254 nm); Initial pH 3.0; 0.1 mM AB1; $H_2O_2$/AB1 = 64 (molar ratio) | Complete discoloration and $X_{TOC}$ = 90–100% ($t$ = 90–120 min) | [31,59] |
| Acid activated Cu-bentonite | Azo-dye acid black 1 | 8 W UVC light; 0.1 mM AB1; 6.4 mM $H_2O_2$; 0.5 g cat/L; pH 3; $T$ = 30 °C; $H_2O_2$/AB1 = 64 (molar ratio) | $X_{AB1}$ = 100% ($t$ = 30 min)<br>$X_{TOC}$ = 85% ($t$ = 120 min) | [32] |
| Fe-laponite | Reactive Red HE-3B | 500 mg/L $H_2O_2$; 1.0 g Fe-Lap-RD/L; 2 × 8 W UVC (254 nm); pH 3.0; 100 mg/L HE-3B; $H_2O_2$/HE-3B = 205.3 (molar ratio) | Complete discoloration ($t$ = 30 min); $X_{TOC}$ = 76% ($t$ = 120 min) | [33] |
| Fe-bentonite | Azo dye Orange II (OII) | 1 × 8 W UVC light (254 nm); 0.2 mM OII; initial pH 6.6; 10 mM $H_2O_2$; 1 $g_{cat}$/L; $H_2O_2$/OII = 50 (molar ratio) | $X_{color}$ = 100% ($t$ = 90 min)<br>$X_{TOC}$ > 65% ($t$ = 120 min) | [60] |
| Fe-bentonite | Azo dye Orange II | 1 × 8 W UVC light (254 nm); 0.2 mM OII; initial pH 3.0; 10 mM $H_2O_2$; 1 g cat/L; $H_2O_2$/OII = 50 (molar ratio) | $X_{color}$ = 100% ($t$ = 60 min)<br>$X_{TOC}$ = 100% ($t$ = 120 min) | [61] |
| Fe-laponite | Azo dye Orange II | 1 × 8 W UVC light (254 nm); 0.2 mM OII; initial solution pH 3.0; 10 mM $H_2O_2$; 1 $g_{cat}$/L; $H_2O_2$/OII = 50 (molar ratio) | $X_{color}$ = 100% ($t$ < 45–60 min); $X_{TOC}$ = 70–90% ($t$ = 90–120 min) | [61,62] |
| Fe-montmorillonite | Reactive brilliant orange X-GN | Visible radiation, halogen lamp ($\lambda \geq 420$ nm); $T$ = 30 °C; pH 3.0; 4.9 mM $H_2O_2$/L; 0.6 $g_{cat}$/L; $\lambda \geq 420$ nm | $X_{color}$ = 98.6%; $X_{TOC}$ = 52.9%; Fe leaching < 1.26% (t = 140 min) | [63] |
| Fe-montmorillonite | Methylene blue (MB) | 4 × 18 W ($\lambda$max = 360 nm); $T$ = 27 °C; 0.2 mM MB; 10 mM $H_2O_2$; 1 $g_{cat}$/L; Initial pH 3.0; $H_2O_2$/MB = 50 (molar ratio) | $X_{MB}$ = 93% ($t$ = 180 min) | [11] |
| Fe-laponite | Monuron and isoproturon (phenyl urea herbicides) | $C_{monuron}$ = 40 ppm; $C_{isoproturon}$ = 25 ppm; 1 $g_{cat}$/L; 10 mM $H_2O_2$; $T$ = 25 °C; pH 3.0; $H_2O_2$/monuron = 49.7; $H_2O_2$/isoproturon = 82.5 (molar ratio) | $X_{TOC} \sim 65\%$ (monuron); $X_{TOC}$ = 87% (isoproturon); ($t$ = 120 min) | [64] |
| Fe-laponite | Ciprofloxacin antibiotic (CFX) | $C_{CFX}$ = 0.15 mM; 60 mM $H_2O_2$; 1.0 $g_{cat}$/L; initial solution pH 3.0; $H_2O_2$/CFX = 400 (molar ratio) | $X_{CFX}$ = 100%; $X_{TOC}$ = 57% ($t$ = 30 min) | [65] |

wastewaters, along with hydroxytyrosol [56]. Actually, the disposal of 30 million $m^3$ of olive mill wastewaters (OMW) every year is a major environmental problem in the Mediterranean countries. OMW have significant pollutant properties, especially due to the high concentration of phenols and polyphenols that are toxic and may inhibit biological treatment. This justifies the studies referred in Table 1 focused on this type of wastewaters, either using synthetic [57] or real [57,58] effluents with AlFe-montmorillonite as catalyst. Besides, AOPs could provide a solution for such environmental problem when used as pre-treatment of OMW by reducing phenol concentration and therefore decreasing their toxicity prior to any biological treatment process.

Dyes have also been the focus of attention by several researchers, as reported in Table 1. It is worth mentioning that more than 700,000 t of about 10,000 types of dyes and pigments are produced every year worldwide [63], from which ca. 20% are directly discharged without any treatment [66]. This yields a significant environmental concern because textile effluents contain several organics, in particular azo-dyes, that are hard to degrade by conventional methods or are even non-biodegradable or toxic to the microorganisms used in the biological units [31,32,63].

The degradation of some herbicides has also deserved special attention, namely monuron and isoproturon (cf. Table 1), which are two of the most important phenyl urea herbicides, with good effectiveness and selectiveness in weed control [64]. It is well known that the use of agrochemicals is a vital necessity for the growing population of the world. For instance, the value of pesticides sold in 2001 was over 40.9 billion USD, the share of herbicides being of 53%

[67]. However, huge amounts of these compounds appear in the water courses, because most of the substance applied (about 98%) is unused by plants and moves through the soil into the groundwater [64]. Monuron has a half life of more than 56 days in river water and up to 170 days in the soil. It is a persistent and bio recalcitrant pollutant [68]. Isoproturon has been found in the effluents of wastewater treatment plants [68]. These herbicides are difficult to remove by a conventional wastewater treatment process, thus justifying the employment of AOPs, namely photo-Fenton-like using Fe-laponite.

Other compounds that received special attention are antibiotics, particularly ciprofloxacin (CFX) (cf. Table 1), a broad-spectrum antibiotic used in human and veterinary medicine. CFX belongs to the class of fluoroquilones (FQs), which currently represent one of the most important classes of antibiotics [65]. Because of their continued use in both human and veterinary medicine, the environmental impact of such antibacterial agents represents a serious concern for the public health due to their potential for migration into the environment (via discharges of wastewater and direct runoff) and the possible development of resistance in pathogens. CFX has been detected at concentrations ranging from μg/L (in untreated hospital sewage) down to ng/L (in secondary wastewater effluents and surface waters) [65,69,70]. The problem is that most of wastewater treatment plants are not designed to completely remove most pharmaceuticals, and consequently they are released into receiving water bodies.

## 2. Effect of the main operating conditions

The photo-Fenton-based processes are affected by several process parameters, as described and exemplified along the following sections.

### 2.1. Effect of the wavelength and power of the radiation source

Before discussing the effect of the wavelength and of the power of radiation, it should be remarked that the promotion of reaction (4) is favored at wavelengths larger than 350 nm [71]. Shorter wavelengths promote the photolysis of hydrogen peroxide, but actually this is not the photo-Fenton reaction. Even more, some authors have reported the use of filters to cut off the radiation with short wavelengths in order to have in their systems exclusively photo-Fenton contribution (e.g. Martínez et al. filter the radiation with $\lambda < 313$ nm [14]), while other authors have reported homogeneous photo-Fenton oxidation under solar irradiation, but this is out of the scope of the present review.

The type of lamp used and its power may affect significantly the performance in the photo-Fenton degradation. As an example, let us mention the work by Iurascu et al. [54], who have tested different types of light sources during phenol degradation with laponite materials. As shown in Fig. 1, better phenol conversion was obtained under irradiation than in the dark (experiment denoted as "Fenton", which was carried out in the same conditions as the others, but in the absence of radiation). Regarding the illuminated systems, the use of UV-C radiation provided much better results, with higher conversion values, for short times of irradiation. Despite the lower power of the adopted UV-C radiation compared to UV-A (Unilux Philips lamps: 15 W UV-C, $\lambda_{max} = 254$ nm, and 40 W UV-A, $\lambda_{max} = 365$ nm, with irradiances of 6 and 16 W/m$^2$ for UV-C and UV-A, respectively), the results obtained were ascribed to the fact that UV-C is absorbed more effectively by the different species present in the system (Fe(III) compounds, phenol and $H_2O_2$). This can thus enhance the photo-Fenton process but also induce the direct photolysis of both $H_2O_2$ to yield HO• (Eq. (7)) and of phenol, leading to its degradation, which explains the conversion noticed

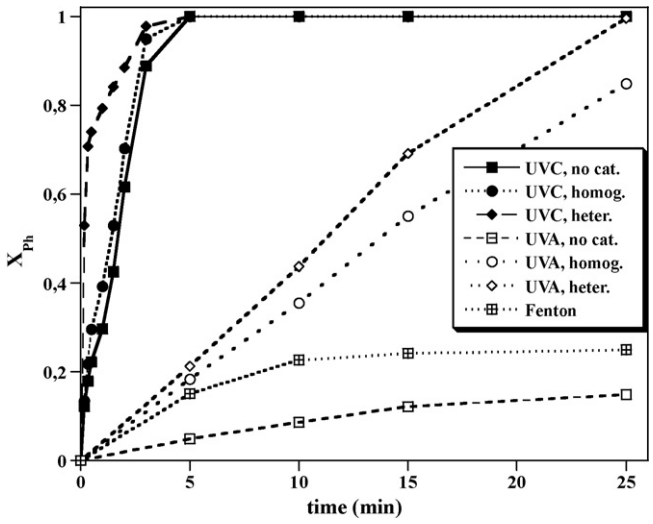


**Fig. 1.** Effect of the light source on phenol conversion ($C_{Fe\text{-}Lap\text{-}TA\text{-}350\ catalyst} = 1$ g/L, $C_{Ph,o} = 1$ mmol/L; $C_{H_2O_2,o} = 50$ mmol/L (molar ratio $H_2O_2$/Ph = 50), pH 3; $T = 30$ °C) [54]. Reprinted from Water Research, 43/5, B. Iurascu, I. Siminiceanu, D. Vione, M.A. Vicente, A. Gil, Phenol degradation in water through a heterogeneous photo-Fenton process catalyzed by Fe-treated laponite. Copyright (2009), with permission from Elsevier.

even in the absence of catalysts (particularly using UV-C radiation).

$$H_2O_2 + h\nu \rightarrow 2HO^{\bullet} \quad (7)$$

The better performances achieved with UVC vs. UVA are in line with other studies [e.g., 31,33], who claimed that UV light wavelength can significantly influence the direct formation of HO• species as well as the photo-reduction rate of $Fe^{3+}$ to $Fe^{2+}$ (cf. Eq. (4)). In particular, several authors have mentioned that the quantum yield of this photo-reduction significantly increases as the UV light wavelength decreases [33], and that $H_2O_2$ does not absorb at all above ~320 nm (and so UVA would not directly take part in decomposing $H_2O_2$ to produce •OH radicals but only in converting $Fe^{3+}$ to $Fe^{2+}$ by photo-reduction) [31]. Nevertheless, the effect of Fe leaching cannot be ignored. In fact, it has been reported that the Fe leaching order is as follows: dark-Fenton < UVA-assisted photo-Fenton < UVC-assisted photo-Fenton, although no reason for this was appointed by the authors [72]. Possibly, the more active is the catalytic system, the higher is the pH decrease, increasing the leaching degree.

Feng et al. have also showed that an increase in the power of the radiation produces an increase in the catalytic activity [33]. This was observed by increasing from 8 to 16 W the power of a 254 nm UV light used in the degradation of the reactive HE-3B dye, finding a significant increase of the TOC removal ratio. When the power of UV light increased a faster photo-reduction of $Fe^{3+}$ to $Fe^{2+}$ was obtained, and, as a consequence, the regeneration rate of $Fe^{2+}$ increases. Accordingly, the number of HO• radicals formed increases substantially, also giving rise to a higher mineralization of the dye.

As indicated, several factors influence the activity of a given system. So, it is common practice to start with "blank" tests, i.e., irradiating the system but in the absence of both catalyst and oxidant (which allows to quantify the extent of direct photolysis), or adding the catalysts but in the absence of both radiation and oxidant (which allows to evaluate the degree of adsorption). As an example, let's focus in the case of the reactive Red HE-3B mineralization with a laponite clay-based Fe nanocomposite (Fe-Lap-RD), although in this case the contributions of these phenomena (direct photolysis and adsorption) are null or almost negligible, respectively (< ca. 5% after 120 min), as shown in Fig. 2 (curves a and b) [33].

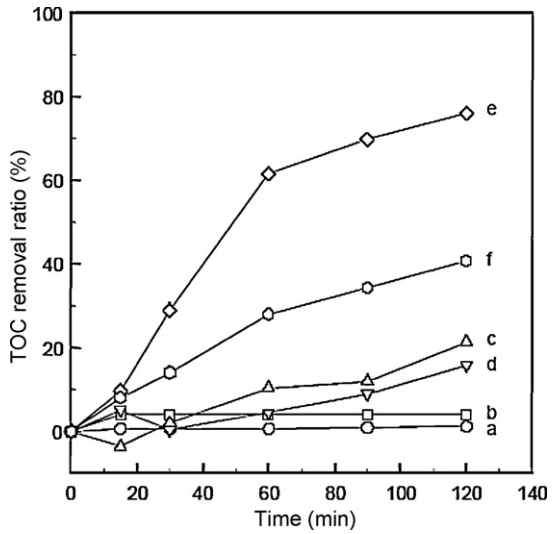


**Fig. 2.** TOC removal of 100 mg/L HE-3B under different conditions: (a) without Fe-Lap-RD catalyst and $H_2O_2$ but only with 2 × 8W UVC, (b) without $H_2O_2$ but with 1.0 g Fe-Lap-RD/L and 2 × 8W UVC, (c) without Fe-Lap-RD catalyst but with 500 mg/L $H_2O_2$ and 2 × 8W UVC, (d) with 1.0 g/L Fe-Lap-RD catalyst and with 500 mg/L $H_2O_2$ in the dark, (e) with 1.0 g/L Fe-Lap-RD catalyst, 500 mg/L $H_2O_2$, and 2 × 8W UVC (molar ratio $H_2O_2$/HE-3B = 205.3) [33]. Reprinted from Water Research, 37/15, J. Feng, X. Hu, P. L. Yue, H. Y. Zhu, G. Q. Lu, Discoloration and mineralization of reactive red HE-3B by heterogeneous photo-Fenton reaction. Copyright (2003), with permission from Elsevier.

### 2.2. Effect of the initial $H_2O_2$ concentration

In a photo-Fenton-based system, the oxidant concentration is a key factor that can significantly influence the degradation of organics. The $H_2O_2$ concentration is directly related to the number of hydroxyl radicals generated, and thus to the performance achieved.

Fig. 3 displays an example of the effect of the hydrogen peroxide dosage, in this case for decolorizing reactive brilliant orange X-GN over iron-pillared montmorillonite [63]. It can be noticed that when increasing the $H_2O_2$ concentration from 2.9 to 9.8 mmol/L ($H_2O_2$/X-GN molar ratio in the range 17.8–60.3), the degradation

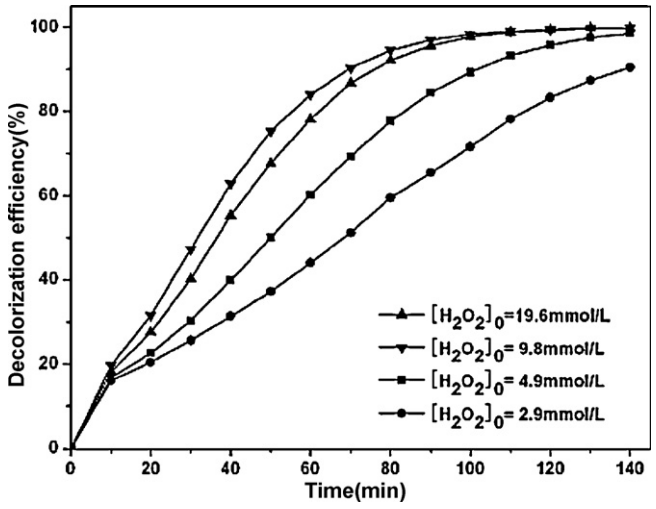


**Fig. 3.** Effect of the $H_2O_2$ dosage on the decolorization of X-GN by heterogeneous photo-Fenton process. The experiments were conducted under the following conditions: [X-GN] = 100 mg/L, Fe-Mt = 0.6 g/L, pH 3, $T$ = 30 °C (molar ratio $H_2O_2$/X-GN = 17.8–120.6) [63]. Reprinted from Journal of Hazardous Materials, 168/2-3, Q. Chen, P. Wu, Y. Li, N. Zhu, Z. Dang, Heterogeneous photo-Fenton photodegradation of reactive brilliant orange X-GN over iron-pillared montmorillonite under visible irradiation. Copyright (2009), with permission from Elsevier.

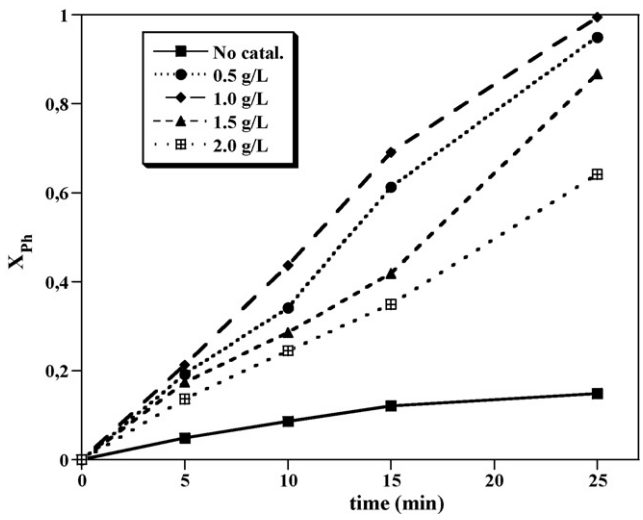


**Fig. 4.** Effect of the catalyst amount on phenol conversion (Fe-Lap-TA-350 catalyst, $C_{Ph,o}$ = 1 mmol/L; $C_{H_2O_2,o}$ = 50 mmol/L (molar ratio $H_2O_2$/Ph = 50), pH 3; $T$ = 30 °C, 40W UV-A lamp) [54]. Reprinted from Water Research, 43/5, B. Iurascu, I. Siminiceanu, D. Vione, M.A. Vicente, A. Gil, Phenol degradation in water through a heterogeneous photo-Fenton process catalyzed by Fe-treated laponite. Copyright (2009), with permission from Elsevier.

efficiency of the dye went up from 65.4% to 95.6% at 90 min. However, when the $H_2O_2$ dosage was above 9.8 mmol/L, the removal of X-GN decreased, although slightly. Nevertheless, this detrimental effect becomes more noticeable at shorter reaction times. This is due to the fact that at higher $H_2O_2$ concentrations scavenging of HO• radicals will occur, as expressed by the following equations [56,63]:

$$H_2O_2 + HO^\bullet \rightarrow HO_2^\bullet + H_2O \quad (8)$$

$$HO_2^\bullet + HO^\bullet \rightarrow H_2O + O_2 \quad (9)$$

It is important to remark that $HO_2^\bullet$ is less reactive than HO•, and thus an increased amount of hydrogen peroxide has a diminishing return on the reaction rate.

A similar behavior, i.e., the existence of an optimum peroxide dose, has also been found during mineralization of reactive dye HE-3B [33] or tyrosol [56]. However, other studies have reported almost no effect of the initial hydrogen peroxide concentration, possibly because the maximum level of efficiency was already attained. This was the case, for instance, of the degradation of phenol (1 mM solution) when $C_{H_2O_2}$ was varied between 20 and 100 mM [54].

If one writes the stoichiometric equation that leads to the complete oxidation of the organic compound by $H_2O_2$, i.e. up to $CO_2$ and $H_2O$, the theoretical [$H_2O_2$]/[organic compound] molar ratio can be determined; however, the reported optimal experimental values (i.e. the real values) are usually much larger (e.g. eight times larger [65]), meaning that an excess of $H_2O_2$ is required to reach the maximum degradation. This means that a significant amount of the oxidant is not effectively used, and thus more appropriate dosage methods are required, as discussed below (cf. section 4.3).

### 2.3. Effect of the catalyst load

Iurascu et al. [54] studied the photo-degradation of phenol with laponite-based materials changing the load of catalyst between 0.5 and 2 g/L, finding an optimum dose of 1 g/L (Fig. 4). By increasing the catalyst dose, higher reaction rates and performances are expected (because it increases the rate of $H_2O_2$ decomposition, hence increasing HO• radical production), but this was noticed only for low doses. The deleterious effect observed for high amounts of catalyst has been attributed to the turbidity of the suspension that

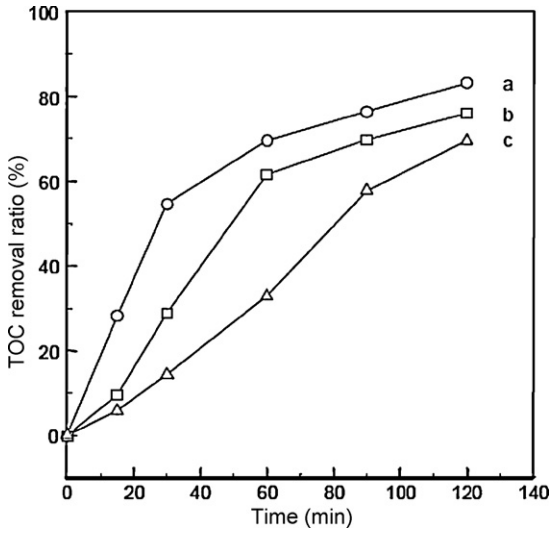


**Fig. 5.** Effect of initial HE-3B concentration on TOC removal ratio. Conditions: 500 mg/L $H_2O_2$, 1.0 g Fe-Lap-RD/L, pH 3.0, 2 × 8W UVC. Initial HE-3B concentration in solution: (a) 50 mg/L, (b) 100 mg/L, and (c) 200 mg/L (molar ratio $H_2O_2$/HE-3B = 102.6–410.6) [33]. Reprinted from Water Research, 37/15, J. Feng, X. Hu, P. L. Yue, H. Y. Zhu, G. Q. Lu, Discoloration and mineralization of reactive red HE-3B by heterogeneous photo-Fenton reaction. Copyright (2003), with permission from Elsevier.

would cause a relevant fraction of the incident radiation to be lost via scattering, not being absorbed and therefore no longer being available to induce the photo-Fenton process [54].

The decrease of the UV light penetration as a consequence of the solution turbidity caused by the small particle size of the catalysts was also reported by other authors (e.g. [31–33,63,65]). Such explanation was interestingly corroborated by Yip et al. by measuring the residual $H_2O_2$ along time, which was smaller for catalyst loads that provided maximum mineralization degrees of the organic compound (dye, in their work) [32]. Other authors attribute the existence of a limiting catalyst dose value (after which reaction rate does not increase) to diffusion limitation phenomenon, causing a decrease of the accessible number of surface active sites [56].

However, the existence of an optimum catalyst dose has not been always documented, and in some cases oxidation performance increased with the amount of catalyst employed [e.g., 64]. But this obviously depends on the range of doses considered, and conditions employed.

### 2.4. Effect of the initial parent compound concentration

Several researchers have investigated the effect of the initial concentration of pollutant, as it is of importance in any process of wastewater treatment. For example, Feng et al. reported the performance reached for the reactive red HE-3B dye degradation varying the initial concentration of the dye from 50 to 200 mg/L [33]. As shown in Fig. 5, the mineralization of HE-3B is more efficient at a lower dye concentration. This phenomenon was associated by the authors with the characteristics of the UV visible absorption spectrum of the dye, which is significant at 254 nm (UVC light tubes, Philips 8W 254 nm, have been used). Therefore, the solution with an initial higher dye concentration will absorb a more significant fraction of the emitted UV light at 254 nm than that with a lower initial concentration, and as a result the number of available photons decreases, leading to a decrease in the formation of HO• radicals [33]. Accordingly, the mineralization ratio of HE-3B decreases as the initial dye concentration increases.

Apart from the author's explanation, it could be also advanced the fact that in these heterogeneous processes the low catalytic

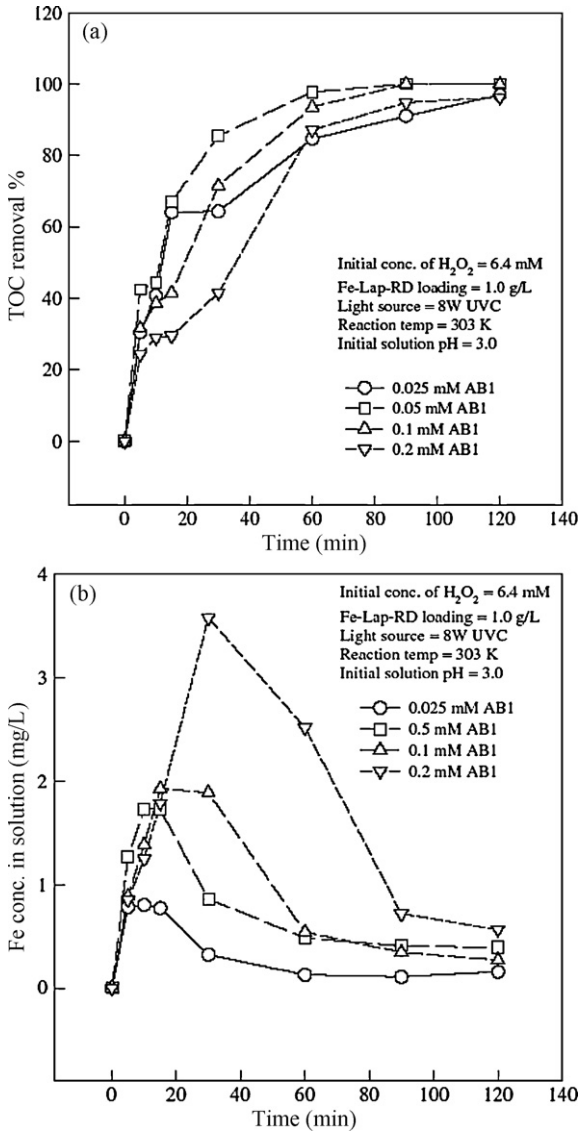


**Fig. 6.** Effect of initial AB1 concentration on (a) TOC removal and (b) Fe concentration in solution (molar ratio $H_2O_2$/AB1 = 32–256) [31]. With kind permission from Springer Science + Business Media: Topics in Catalysis, Photo-assisted Fenton mineralization of an azo-dye acid black 1 using a modified laponite clay-based Fe nanocomposite as a heterogeneous catalyst, 33, 2005, 233, O.S.N. Sum, J. Feng, X. Hu, P.L. Yue, copyright notice displayed with material.

activity at high pollutant doses can be ascribed to the existence of an induction period. This induction period is possibly related with the formation of intermediate oxidation products, which trap radicals, as reported during phenol oxidation [51]. For higher pollutants doses such intermediates are formed in larger concentrations. When they disappear, the activity of the metal-system increases immediately.

Notwithstanding, in a more recent study by the same group the authors arrived to different results [31]. As shown in Fig. 6a, during the azo-dye acid black 1 (AB1) degradation the TOC removal after a given irradiation time is not directly proportional to the diminution of the initial dye concentration. To explain this phenomenon, the Fe ion concentration in solution as a function of reaction time was measured for the different experiments (Fig. 6b). It is clear that the peak of Fe concentration increases with the initial concentration of AB1. Thus, the dye concentration can directly influence the concentration of Fe ion leaching from the modified laponite catalyst (Fe-Lap-RD). With the smaller Fe concentration, the degradation of

0.025 mM AB1 can be considered to be fully caused by the heterogeneous oxidation (low Fe leaching), so that the TOC removal rate is slower than the combined heterogeneous and homogeneous oxidations [31]. In contrast, the higher concentration of AB1 promotes higher Fe ion leaching from the Fe-Lap-RD due to the higher amount of acidic products generated; thus, the combined heterogeneous and homogeneous oxidations cause a faster TOC removal. However, if the dye concentration is too high (0.2 mM), the color will affect the UV light penetration depth, causing a slower oxidation. These facts lead to the existence of a trade-off, and so TOC removal is at fastest rate when an intermediate (0.05 mM) AB1 concentration is employed (Fig. 6a). These authors also put into evidence the importance of measuring the amount of Fe leached from the support, because the homogenous process may play a role in the overall performance.

It is worth noting that the existence of a maximum in the Fe concentration reported in Fig. 6b (and also in several other studies available in the literature) was ascribed to the fact that some reaction intermediates such as oxalate anions can capture Fe ions and form Fe complexes, increasing the amount of iron in the solution. When the concentration of the intermediates attains a maximum, the Fe concentration also exhibits a peak value, while when the intermediates are mineralized into $CO_2$ and $H_2O$ (longer reaction times), the Fe ions return to the surface of the pillared clay support [61].

The behavior shown before regarding the existence of an inverse proportionality between pollutants concentration and oxidation efficiency is quite typical for the photocatalytic degradation of many organic compounds. Nevertheless, the reasons attributed to such trend vary from work to work. For instance, Azabou et al. found that the apparent rate constant in the degradation of phenolic compounds present in olive mill wastewaters (e.g., hydroxytyrosol or tyrosol) decreases with increasing initial pollutant concentration [57]. According to them, the reaction occurs at the surface of (Al–Fe)PILC catalyst between the HO radicals generated at the active sites and the phenol molecules adsorbed on the surface (Langmuir-Hinshelwood-type mechanism). Thus, when the initial phenol concentration is too high, the number of active sites available is decreased by the phenolic molecules, due to their competitive adsorption on the catalyst surface [57].

Yip et al. have shown that the inverse proportionality between dye concentrations and reaction rates only applies if the hydrogen peroxide/dye molar ratio is adjusted and kept constant, for instance according to the theoretical molar ratio (as given by the reaction that leads to complete mineralization of the pollutant) [32].

However, in other studies no effect of the initial concentration of pollutant was noticed, for instance when the initial phenol concentration was varied between 0.5 and 1.5 mmol/L, probably because this effect is masked by those caused by other variables of the system or because the range is too short [54].

### 2.5. Effect of the initial pH

The pH of the medium is a crucial operating parameter, as it directly affects not only the photo-catalytic performance but also the extent of Fe leaching from the support (and thus the long-term stability of the catalyst). There is a general agreement in the literature about the optimal pH being close to 3, which is also a typical value for the homogeneous photo-Fenton process [61]. In homogeneous phase, at pH 2.8 approximately half of the Fe ion is present as $Fe^{3+}$ and half as the complex ion $Fe(OH)^{2+}$, which are the photoactive species (cf. Eq. (4)). Lower values of pH results in declining the concentration of $Fe(OH)^{2+}$, while higher pH values results in precipitation of oxyhydroxides [73], both negatively affecting catalytic performance. The pH of the reaction medium also affects the $HO^{\bullet}$ radicals concentration [30]; at a pH below 3 the scavenging

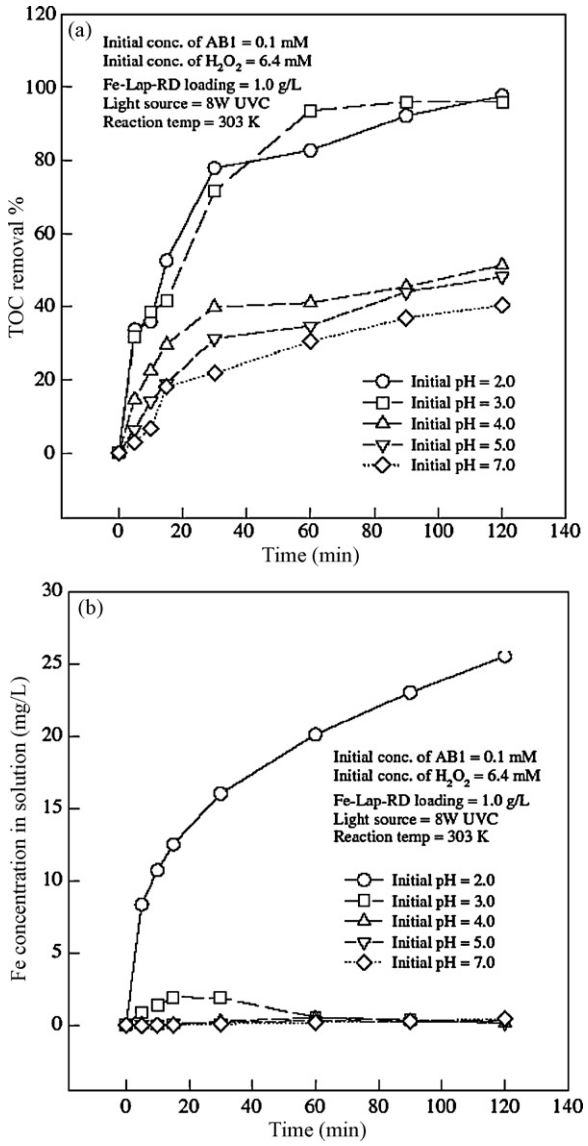


**Fig. 7.** Effect of initial pH of the solution on (a) TOC removal and (b) Fe leaching during degradation of acid black 1 (molar ratio $H_2O_2$/AB1 = 64) [31]. With kind permission from Springer Science + Business Media: Topics in Catalysis, Photo-assisted Fenton mineralization of an azo-dye acid black 1 using a modified laponite clay-based Fe nanocomposite as a heterogeneous catalyst, 33, 2005, 233, O.S.N. Sum, J. Feng, X. Hu, P.L. Yue, copyright notice displayed with material.

effect of these radicals by $H^+$ is severe, while for pH > 3 the formation of hydroxyl radicals slows down due to the hydrolysis of Fe(III) and the precipitation of FeOOH from the solution, as mentioned above. Another issue that is pH-dependent is the hydrogen peroxide stability, which also explains why a decrease of performance is often found for pH values below 3. In such circumstances, formation of $H_3O_2^+$ occurs, enhancing the stability of $H_2O_2$ and inhibiting the generation of HO radicals [63]. Besides, the rate of undesirable $H_2O_2$ decomposition shows the lowest value at pH 3.0 [56].

Fig. 7a illustrates typical results for the effect of the pH, in this case for the acid black 1 degradation [31]. It is found that the TOC removal decreases with increasing the initial pH of the solution, emphasizing that the photo-assisted Fenton reaction is inefficient at solution pH higher than 3.0. When the initial solution pH is 2.0, the TOC removal is close to that reached when the pH is 3.0. To explain this issue, Sum and co-workers have measured the Fe concentration in solution for all these experiments, and the results are illustrated in Fig. 7b [31]. It is observed that the Fe ion leach-

ing from the heterogeneous support (Fe-based laponite) becomes severe when the initial pH of the solution is 2.0. Therefore, under such pH value TOC removal is fast because of the homogeneous contribution of leached iron. However, and as pointed by the authors, it should be stressed that when a high concentration of Fe ions is present in solution, a post-treatment is necessary to remove them from the treated water. Therefore, the optimum solution pH recommended is 3.0. Once again, and as highlighted in the previous section, these results put into evidence the importance of measuring also the level of Fe leached from the support, because the homogenous process may play an important role.

Similar conclusions were obtained during Orange II discoloration and mineralization with either bentonite- or laponite-based catalysts [61]. Here, an initial pH of 3.0 showed again to be the optimum value, performances decreasing for lower or higher values. In this study, the authors highlighted the importance of the excellent performance of these materials at higher pHs, in some cases even under neutral conditions. This is also found in the work from Sum et al. (see Fig. 7), because the Fe-based laponite used in this work also displays a reasonable good photocatalytic activity and negligible Fe leaching at an initial solution pH close to 7, which makes pillared clay-based solids good candidates for preparing long-term stable catalysts [31]. In addition, the photo-Fenton treatment of wastewaters without pre-adjusting their pH might also become feasible, because industrial organic contaminated wastewaters often have pH around 7 [32]. Moreover, under such conditions the need of special materials for the reactor (resistant to corrosion) is avoided.

The reason for the good photocatalytic activity of these materials when the initial pH of the solution is 6.6–7.0 has been attributed by some authors to the decrease of the pH along the oxidation (e.g., [60]). This pH change results from the formation of acidic intermediates and products. For example, muconic, maleic, succinic, malonic, oxalic, formic and acetic acids have been detected during degradation of phenol and phenolic compounds [74], and the own final $CO_2$ is an acid itself. Thus, a reasonably good photocatalytic activity has been reported when using $Fe^{3+}$-doped $TiO_2$ or Fe-bentonite nanocatalysts for the degradation of Orange II, even when the initial solution pH is almost neutral, and with only a negligible loss of Fe ions from the supports [60]. Similar results were obtained by Najjar et al. during tyrosol oxidation [56]. However, other authors have found very similar performances at initial pHs ranging from 3.0 to 6.0 [11]. According to them, the effects above described for homogeneous photo-Fenton processes when pH is below or above 3.0 are strongly attenuated in heterogeneous systems, since immobilized Fe(III) species can not be easily transformed into less photoactive materials, i.e., $[Fe(H_2O)_6]^{3+}$ at lower pH and $Fe(OH)_3$ at higher pH. Furthermore, the stabilization of iron oxide pillars may also be attributable to interactions with the clay sheet [11]. Najjar and co-workers also state that the reasonable activity under initial pH close to 7 may correspond to the specific environment of ferric species in the pillars, where the speciation of $Fe^{3+}$ is certainly different from that in solutions [56]. These authors propose that some active iron species can exist even at neutral pH and they can establish an effective Fenton-type redox system.

In any case, several other studies have also reported good performances at pH ~3 in heterogeneous systems, namely in the degradation of reactive brilliant orange X-GN [63], ciprofloxacin [65], or acid back 1, the later with either Fe/or Cu/acid-activated bentonites [32].

As discussed below (cf. section 3.3), Cu-based catalysts are particularly promising when aiming operation at higher pHs because Cu is less sensitive than Fe to changes in this variable, being thus able to hold their activity in a wider pH range [32].

Thus, in conclusion, an initial pH of ~3 has been established is most studies. In these conditions, the medium is not too acidic to provoke excessive leaching of Fe from the catalysts but not so high to provoke important decrease of activity. Nevertheless, and as reported above, some efforts have been devoted to the study of this reaction at neutral medium; other works also addressed this issue aiming to consider the application of metal-clays in reactions at nearly neutral or even basic conditions [75–78].

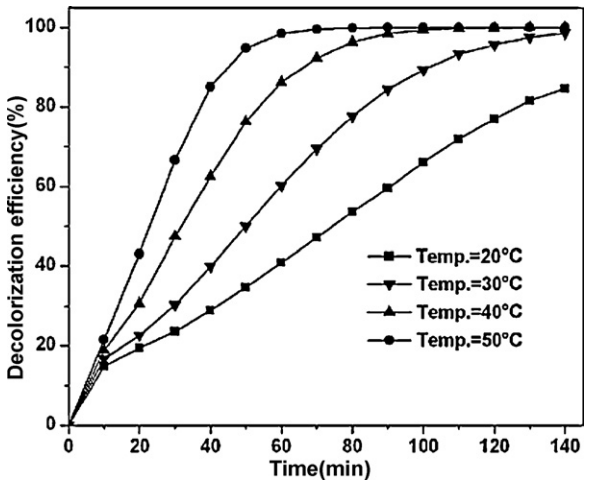


**Fig. 8.** Effect of temperature on the decolorization of X-GN by heterogeneous photo-Fenton process. The experiments were conducted under the following conditions: [X-GN] = 100 mg/L, $[H_2O_2]_o$ = 4.9 mmol/L, catalyst = 0.6 g/L, pH 3 (molar ratio $H_2O_2$/X-GN = 30.2) [63]. Reprinted from Journal of Hazardous Materials, 168/2-3, Q. Chen, P. Wu, Y. Li, N. Zhu, Z. Dang, Heterogeneous photo-Fenton photodegradation of reactive brilliant orange X-GN over iron-pillared montmorillonite under visible irradiation. Copyright (2009), with permission from Elsevier.

### 2.6. Effect of the temperature

Reaction temperature is another important process parameter, but rarely addressed in the literature dealing with the use of PILCs in the photo-Fenton process. A scarce example is given in the very recent work by Chen et al., focused on the degradation of reactive brilliant orange X-GN over iron-pillared montmorillonite [63]. As shown in Fig. 8, higher temperatures (in the range 20–50 °C) accelerated the decolorization of the dye because the rate of $HO^{\bullet}$ generation increases with temperature (Arrhenius dependence of the rate constants). It is noteworthy that in the same temperature range, thermal decomposition of the dye was nearly negligible, amounting up to only 1.7% after 140 min (at 50 °C) [63].

Sum et al. also analyzed the effect of temperature (in the range 30–75 °C) on the degradation of azo-dye acid black 1 [31]. They found that, in general, the initial TOC removal rate increases with reaction temperature, particularly in the first 30 min. This was attributed to the increase of both the collision frequency of molecules on the surface of the catalyst and to the fraction of molecules that possesses energy in excess of the activation [31]. However, they found that the TOC removal after 2 h reaction is similar under the range of studied temperature. The results obtained allowed them to fit the data to a pseudo first-order rate equation (although only the values of the first 15 min have been used), as described below (cf. Section 6.3), and to compute the apparent activation energy: 24.71 kJ/mol [31]. A value for this parameter of only 10.86 kJ/mol was obtained by Najjar et al. during tyrosol degradation [56].

It is however common to find reported an optimum value for temperature, usually around 30 °C, because above this point $H_2O_2$ tends to be thermally decomposed into $H_2O$ and $O_2$, and is subjected to a scavenging effect [32]. Nevertheless, this has not been always observed and in some cases the effect of temperature in the catalytic process prevails. The reason is that the activity of thermal

Fenton/photo-Fenton processes is remarkable for values around 50–75 °C [79], or even higher (e.g. 100 °C, but for pressurized systems) [80].

### 2.7. Heterogeneous vs. homogenous process

The importance of the relative contribution of the heterogeneous vs. the homogeneous process is another important issue to analyze in order to determine if the degradation is due to oxidation by radicals coming from the breakage of $H_2O_2$ catalyzed by the clay-based catalyst or by the Fe ions in solution that have been leached out from the support in acidic solution. As has been already indicated, the leaching of iron from the solid catalysts is strongly influenced by the pH, the temperature, the intermediate products, etc., making difficult to predict the homogeneous contribution.

Fig. 1 puts this issue into evidence for the case of phenol degradation. Under both UV-A and UV-C conditions it can be observed that the degradation rate order is as follows: no catalyst < homogeneous conditions < heterogeneous conditions [54]. In this study, the amount of Fe (2 mg $Fe^{3+}$/L) dissolved in solution in the homogenous run was higher but comparable to the amount of iron leached from the Fe-Laponite heterogeneous system, which was never higher than 1 mg Fe/L. This allows checking that the degradation is mainly caused by the solid Fe species present in the clay rather than by Fe species leached into the solution [54].

Fig. 2 provides another example, illustrating the results obtained for the mineralization of reactive Red HE-3B with a laponite clay-based Fe nanocomposite (Fe-Lap-RD) [33]. When comparing curves e and f, but taking into account the effective levels of leaching (<2 mg $Fe^{3+}$/L), these authors concluded that the mineralization of the dye is mainly due to oxidation by HO radicals coming from $H_2O_2$ catalyzed by the Fe-Lap-RD instead of by Fe ions leached out from that catalyst. Similar conclusions were obtained during the degradation of azo-dye Orange II [62]. In a more recent study from the same group, using the same laponite based catalyst but focused on azo-dye acid black 1 degradation [31], almost no difference was noticeable between those curves; so, in this case, the performance of the heterogeneous catalyst in the discoloration process is similar to that of 2 mg $Fe^{3+}$/L homogeneous system.

Several other studies can be found in the literature addressing this issue [e.g., 63]. However, it is often hard to quantify the effective contribution of the homogeneous process, because the amount of Fe leached varies along time. One way to circumvent this problem could be the use of a semi-continuous reactor, in which the Fe solution is added continuously. The flow rate and concentration of Fe in this solution have however to be adjusted to simulate as close as possible the leaching in the batch heterogeneous experiment. In addition, care must be taken to not change significantly the reaction volume along time.

## 3. Effect of type of catalyst/synthesis conditions

In this section, we will briefly refer some studies in which different pillared clay-based materials have been employed for a given catalytic application. To explain the different performances, the physical and chemical characterization of the materials is then of crucial importance.

### 3.1. Effect of thermal aging

Sum et al. [59] prepared a series of laponite-based Fe-nanocomposites (Fe-Lap-RD) under different conditions, particularly with or without thermal aging treatment (samples are denoted as TA or WTA, respectively). The numbers in the reference of the samples indicate the calcination temperature employed (e.g., 523 K). Fig. 9a shows the mineralization degrees attained during

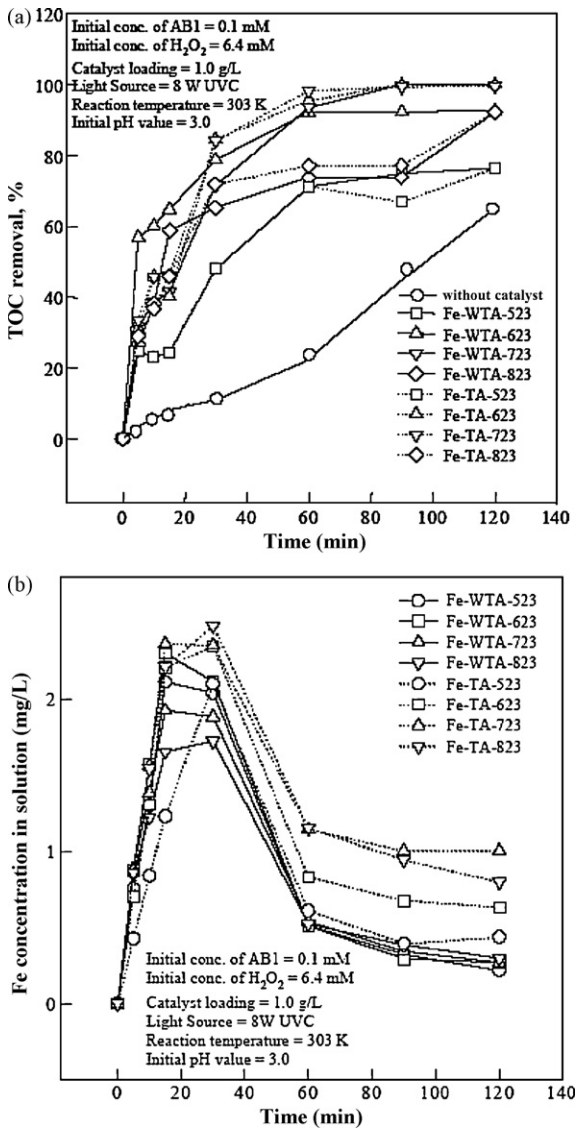


**Fig. 9.** Evolution of TOC removal (a) and Fe concentration in solution (b) for different Fe-Laponite-RD nanocatalysts during acid black 1 degradation (molar ratio $H_2O_2$/AB1 = 64) [59]. Reprinted from Chemical Engineering Science, 59/22-23, O.S.N. Sum, J. Feng, X. Hu, P.L. Yue, Pillared laponite clay-based Fe nanocomposites as heterogeneous catalysts for photo-Fenton degradation of acid black 1. Copyright (2004), with permission from Elsevier.

the photo-Fenton degradation of acid black 1 while Fig. 9b refers to the levels of Fe leached into the solution. As remarked by the authors, when the Fe-Lap-RD nanocatalysts are synthesized under the calcination temperature of 723 K, 100% TOC removal is achieved after 90 min, independently of using thermal aging or not. If one looks at the levels of Fe in solution, particularly at 2 h of reaction time, Fig. 9b evidences that Fe leaching from the samples prepared with thermal aging (TA) is always higher than that from materials prepared without thermal treatment (WTA).

These results were justified on the basis of the characterization data [59]. Catalysts prepared without thermal aging have larger specific surface areas and smaller mesopore volumes than those submitted to thermal ageing, in spite the latter contain higher amounts of Fe (as evidenced by XRF and XPS). This could explain the higher Fe levels in solution for TA samples. Finally, the XRD patterns revealed that highly magnetic $Fe_2O_3$ maghemite-Q and hematite were formed in Fe-WTA and Fe-TA systems, respectively. Thus, Fe-WTA-723 solid, composed of maghemite-Q crystalline form of

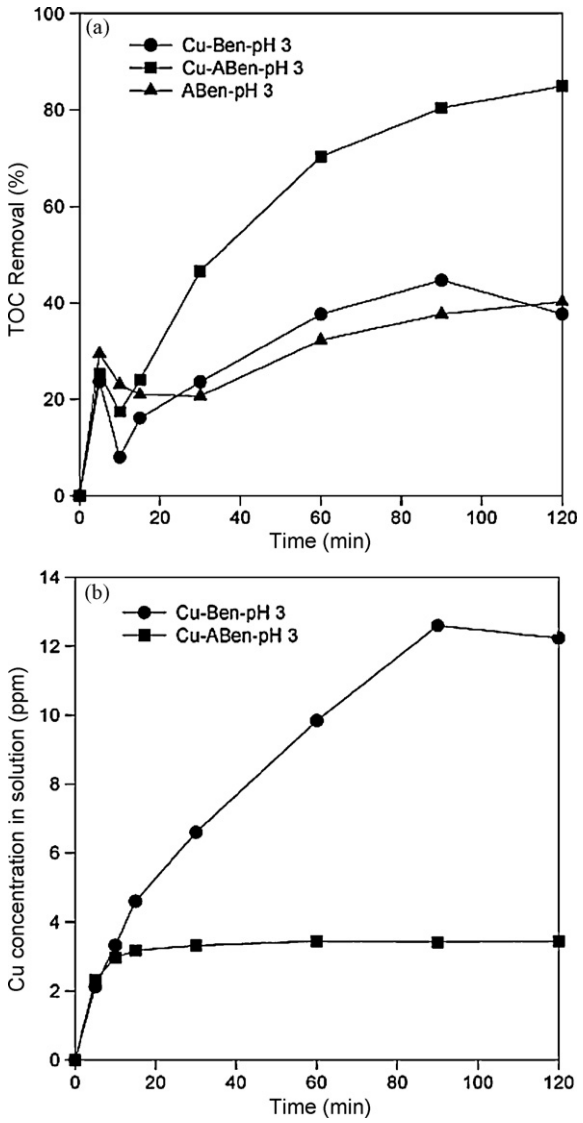


**Fig. 10.** Evolution of TOC removal (a) and Cu concentration in solution (b) along time during Acid Black 1 photo-Fenton-like degradation with different catalysts. Reprinted with permission from [32]. Copyright 2005 American Chemical Society.

$Fe_2O_3$, is the most effective and chemically stable photo-catalyst, being a promising heterogeneous nanocatalyst [59].

### 3.2. Effect of acid treatment

This issue was dealt with in an interesting work by Yip et al. [32], where a Cu/clay catalyst was synthesized by dispersing copper onto the surface of bentonite through chemical vapor deposition (CVD). Copper has been selected as the photo-Fenton reagent instead of Fe due to its ability to keep the catalytic activity at pH around 7, allowing the treatment of industrial organic contaminated wastewater without the requirement of pH adjustment. Several samples were then tested in the photo-Fenton-like oxidation of Acid Black 1 (AB1): Cu/acid-activated bentonite clay (denoted as Cu-ABen), Cu deposited onto the bentonite but without acid activation (denoted as Cu-Ben), and acid-activated bentonite without Cu deposition (ABen) [32]. Results shown in Fig. 10a illustrate that the photo-Fenton-like oxidation of AB1 catalyzed by Cu-ABen was much faster than that reached by the other samples. This behavior was ascribed to the increase in the number of active sites on the acid-activated surface of the bentonite clay [32]. Besides, another important characteristic of the acid activated solid is the minimization of Cu leaching (Fig. 10b). This behavior was attributed to the formation of a monolayer of sulfonate functional groups on the bentonite surface during the acid treatment by $H_2SO_4$. Hence, during CVD, Cu was attached on the surface via those groups. Compared to Cu-Ben, these specific surface functional groups on Cu-ABen enable copper to anchor onto the surface more firmly. The surface modification that leads to leaching minimization was only achieved by the sulfonate groups that are specifically provided by $H_2SO_4$, as evidenced by further experiments with other acids (HCl and $HNO_3$) at different concentrations [32].

### 3.3. Effect of copper

One important advantage of using copper was already addressed: it allows operation at higher pH because it is less sensitive than Fe, being thus able to hold activity in a wider pH range [32]. Furthermore, some authors reported increased catalytic activity with the Cu content in Cu,Al-PILCs. This was also the case in mixed Fe,Cu,Al-clays that were prepared from Ca-montmorillonite by Timofeeva et al. [52] and subsequently tested in the wet peroxide oxidation of phenol. It was concluded that the textural properties (total surface area, micropore volume and interlayer distance) of Fe,Cu,Al-containing clays can be controlled by the Fe/Cu ratio of the pillaring solution and nature of polyoxocation. Besides, the introduction of copper ions results in catalytic reaction acceleration (also revealed by a decrease in the induction period) that was interpreted in terms of the increase of radical generation rate, leading to a different reaction mechanism when comparing Fe- vs. Cu-containing systems [52]. Even so, the better catalytic performance of the mixed material is due to the presence of both species, Fe and Cu, and so to their joint action towards increasing radical generation.

### 3.4. Effect of particle size

Conventional methods use a mineral's clay fraction with particles size typically <2 μm for the preparation of PILCs [11]. The separation of the clay fraction from the starting raw mineral, carried out by dispersion-decantation, is however an expensive and time-consuming process. With this in mind, De León et al. [11] decided to separate two fractions with different particle size of an abundant Uruguayan montmorillonitic clay and test them in the photo-Fenton discoloration of methylene blue. The samples were selected prior to pillaring, ranging below 250 μm and within the range of 250–450 μm. Both catalysts proved to be microporous solids with a significant specific surface area (212 and 140 $m^2/g$, respectively), which justified the significant amounts of dye removed by simple adsorption (63% vs. 52% after 3 h). Thus, an improvement of catalyst textural parameters (higher specific surface area and specific pore volume) and an increase in catalytic activity was found for the smaller-sized particle fraction of the starting mineral [11].

## 4. Some technological issues

With this section we aim to emphasize the importance of technical aspects that were not yet addressed when aiming the implementation of a heterogeneous photo-Fenton process.

### 4.1. Catalyst stability

The stability of a PILC-based catalyst is directly related to the leaching of the metal species, which in turn is affected by the operating conditions employed. This was already addressed along this review, particularly in what concerns the effect of the pH. The effect of the other operating conditions on the level of leaching has been

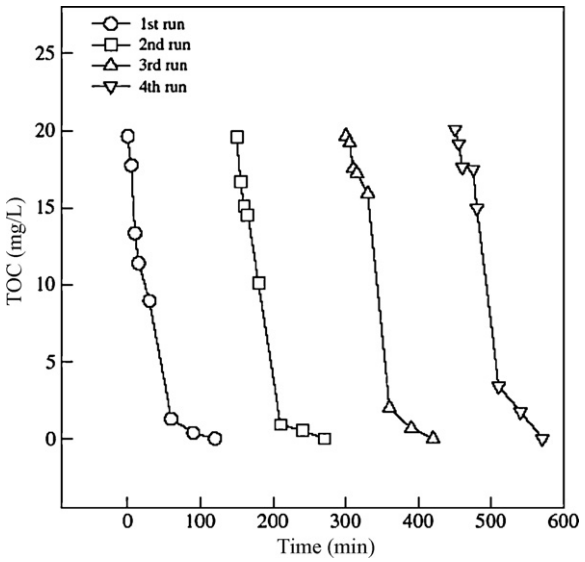


**Fig. 11.** TOC evolution as a function of irradiation time up to four runs in the degradation of AB1 over a Fe-laponite catalyst [31]. With kind permission from Springer Science + Business Media: Topics in Catalysis, Photo-assisted Fenton mineralization of an azo-dye acid black 1 using a modified laponite clay-based Fe nanocomposite as a heterogeneous catalyst, 33, 2005, 233, O.S.N. Sum, J. Feng, X. Hu, P.L. Yue, copyright notice displayed with material.

discussed by Najjar et al. [56]. These authors found that, in general, iron leaching increases with temperature, while by increasing hydrogen peroxide concentration, just a slight increase of leaching was observed; increasing the catalyst loading led to a decrease of iron solubilisation. Their data suggest that the leaching of active species is not a simple dissolution process only related to the acidic nature of aqueous solutions, but it actually seems to proceed by a more complex mechanism in which the ratio peroxide:active species within the course of the catalytic run plays an essential role. Finally, they remarked that the parent compound (tyrosol, in their study) also influences the complex mechanism of iron leaching [56].

The long-term stability of a catalyst is a key issue for its industrial application, apart from the photo-catalytic activity (and price). For this reason, it is common practice try to recover the catalyst after each run and reuse it in several consecutive cycles (when tested in a slurry batch reactor). This was also done, for instance, by Hu and co-workers, as shown in Fig. 11 [31]. These authors remarked that the photocatalytic activity of the Fe-Lap-RD (Fe-laponite) material remains stable in each cycle, with a complete TOC removal being achieved in each run after 2 h. They concluded that the Fe-Lap-RD has a great potential to be used in the total mineralization of AB1 [31] or Orange II degradation [62].

However, as in these studies from Hu and co-workers, the number of cycles is rather limited in most of the works found in the literature, which does not effectively prove the long-term stability of the catalysts. Other methodologies are therefore definitively required.

Yip et al. have also re-used their catalyst along 4 cycles, but in this case a slight decrease in TOC removal was observed after each run, as well as in the adsorption capacity (attributed to the occupancy of the active surface or active sites by the organic dye molecules that were adsorbed on the surface previously and remained undestroyed) [32]. As the pillared clay is an economical catalytic material that can be produced efficiently, the authors considered acceptable to reuse it for 3–4 cycles before rejecting it [32]. This is in our opinion questionable, at least from the environmental point of view, but certainly reactivation studies could be considered in the future for trying to restore the catalyst activity. Some authors have already used this approach, oxidizing the organic species adsorbed on the active sites of the catalyst by an intermediate calcination step [56]. Alternatively, one can fit the operating conditions along the operation, e.g. increasing the temperature, to compensate the activity decay, as suggested previously [36].

Another issue which is worth mentioning is the full characterization of the catalyst, before and after reaction, employing different physical-chemical techniques. This allows identifying, for instance, if there is any change in the Fe content in the bulk or on the surface (by XRF/ICP or XPS, respectively), if the specific surface area changes (BET), or even if the crystalline forms or oxidation states are affected by the oxidation process (by XRD or XPS, respectively). This was done in the studies already commented from Hu and co-workers [31,62], who concluded that leaching of Fe from the laponite clay is negligible, that the crystalline clusters remain stable after four runs and that the binding energy of Fe has either not changed [31] or increased [62]. In the later case, the authors state that the fact that more positive Fe ions are present on the surface of the clay after reaction provides solid evidence that the $Fe_2O_3$ in Fe-Lap-RD indeed participated in oxidation–reduction reactions during the photo-assisted degradation of the dye, Orange II [62]. Very recently, when using modified laponite clay-based nanocomposites during photo-Fenton's oxidation of ciprofloxacin, Bobu et al. also did not detect important changes in the bulk and surface contents of Fe after reaction, neither on the oxidation state of Fe (as inferred from XPS spectra) [65]. So, they anticipated that their catalyst could have a long-term stability for the degradation and mineralization of ciprofloxacin.

### 4.2. Use of fixed-bed reactors

In general, mostly two types of heterogeneous photo-Fenton reactors have been used. One of them employs the suspended catalyst (slurry reactor, in batch or continuous operation), and the other is the fixed-bed mode (the reader should however notice that this approach differs from the classical packed bed). Most studies reported in the literature adopted the first option. However, this requires in practice further separation of the catalyst from the reaction solution after the photochemical treatment, for instance by sedimentation. With this is mind, Feng et al. decided to explore the possibility of using clay-based Fe nanocomposite films, in which the catalysts were coated on the inner wall surface of a stainless steel photo-reactor through the thermal spray method (cf. Fig. 12) [72]. The films were then tested in the photo-Fenton degradation of an azo dye (Orange II) in the presence of UVC light and $H_2O_2$ and the performance compared to that achieved by the corresponding suspended Fe-bentonite (Fe-B) catalyst (1.0 g/L). Although slower decolorization and mineralization kinetics were noticed when using the film (which was attributed by the authors to a decreased specific area in the film), smaller amounts of Fe leached into solution were also observed [72]. However, this comparison is not really effective because the amount of catalyst in each run can be different—data not provided in their paper. Even so, this study puts into evidence the possibility of employing similar technologies, but further studies are required.

### 4.3. Mode of $H_2O_2$ addition

The strategy of the oxidant (hydrogen peroxide) addition is an important issue to consider when optimizing the organic degradation, as nicely shown by Hu and co-workers [32]. To prevent scavenging that often occurs at excessive hydrogen peroxide doses (cf. Eq. (8)), the $H_2O_2$ load was divided into two doses: 80% of the required amount for the theoretical complete mineralization of the pollutant (acid black 1) was added prior to the reaction beginning, while the remaining 20% was added at $t = 15$ min (cf. Fig. 13a). Com-

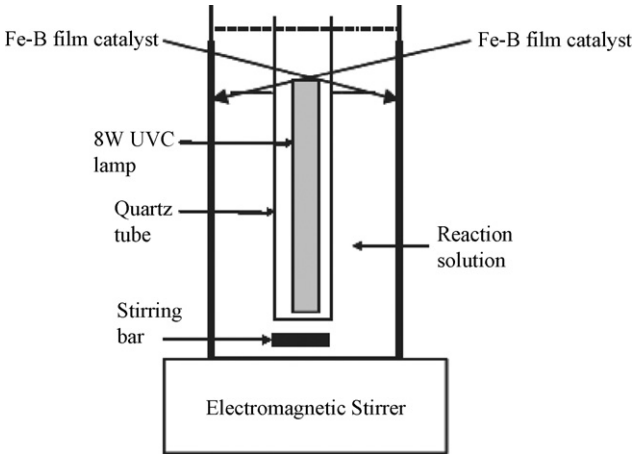


**Fig. 12.** Experimental set-up of the photo-reactor coated with a Fe-bentonite coated catalyst film for the degradation of Orange II [72]. Reprinted from Water Research, 39/1, J. Feng, X. Hu, P.L. Yue, Discoloration and mineralization of Orange II by using a bentonite clay-based Fe nanocomposite film as a heterogeneous photo-Fenton catalyst. Copyright (2005), with permission from Elsevier.

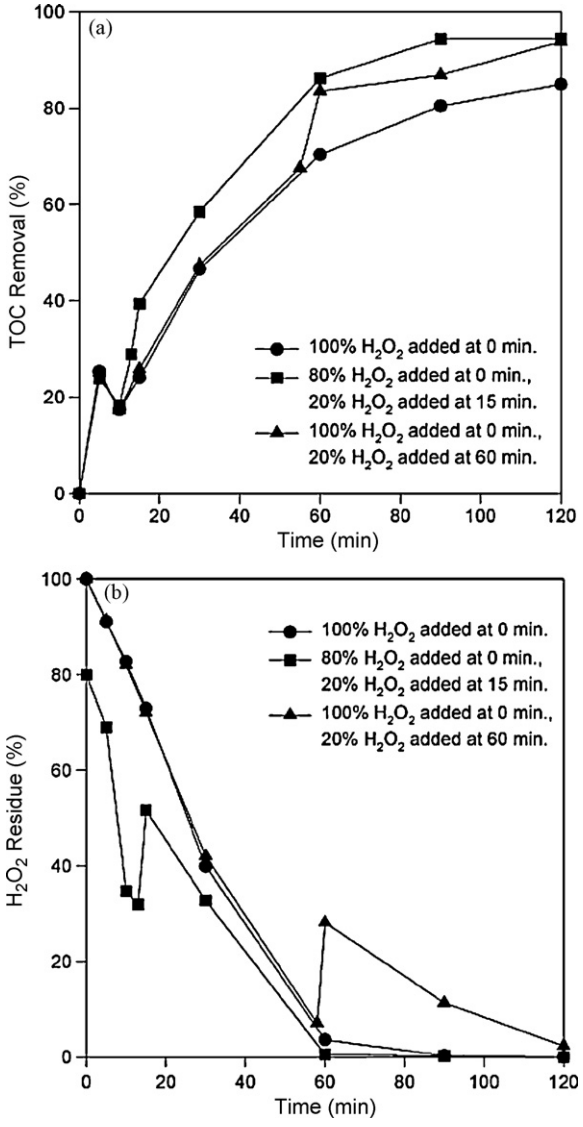


**Fig. 13.** Evolution of TOC removal (a) and $H_2O_2$ residue (b) during AB1 degradation for different $H_2O_2$ dosage strategies. Reprinted with permission from [32]. Copyright 2005 American Chemical Society.

pared to the run in which 100% of the $H_2O_2$ dose was added at $t = 0$, a positive effect in terms of TOC removal was obtained, being particularly notable at the time of the 20% addition (15 min). With less $H_2O_2$ supplied, the added 80% dose is able to bypass the scavenging effect so that the generated HO radicals only target the organic dye compound. The addition of the remaining dose (20%) of $H_2O_2$ at $t = 15$ min continued the organic oxidation and maintained the TOC removal at a higher level. Another attempt was made to boost up the TOC removal by providing excessive $H_2O_2$ at 60 min, when all the $H_2O_2$ was already consumed (Fig. 13b). The results in Fig. 13a show that there was a sharp increase in the TOC removal at 60 min when the excess 20% $H_2O_2$ was added, resulting in a comparable TOC removal at 120 min as the one achieved by splitting the required dosage into a 8:2 ratio. Because the addition of excess $H_2O_2$ should be avoided due to higher chemical cost, it was concluded that the strategy of splitting the required dosage of $H_2O_2$ could minimize the scavenging effect, increasing also TOC removal, being therefore preferred [32].

### 4.4. Use of visible radiation

In the studies reported so far, attention has been mostly focused on the application of the heterogeneous photo-Fenton process making use of UV irradiation. However, the ultraviolet band occupies only 3–5% of the solar light energy that reaches the Earth; moreover, artificial ultraviolet apparatus typically consume large quantities of electrical power, which limits the industrial application [81]. Therefore, an important issue in the heterogeneous photo-Fenton process is to develop catalysts that use sunlight or visible light irradiation instead of UV only as the light source for wastewater treatment. In this sense, Chen et al. synthesized an iron-pillared montmorillonite (Fe-Mt) catalyst that revealed to be particularly efficient under visible light irradiation ($\lambda \geq 420$ nm, provided by a halogen lamp and appropriate filters) for decolorization of reactive brilliant orange X-GN [63]. Such capability can be ascribed to the significant absorption in visible light region up to 600 nm, as evidenced by the catalyst UV-Vis diffuse reflectance spectrum.

Aiming the heterogeneous photo-Fenton process large-scale implementation, other materials, with a wide absorption range are required, which can be obtained for instance by doping.

### 4.5. Environmental impact and integration with biological processes

An important aspect to take into account is the environmental impact of the treatment process, namely in terms of toxicity of the oxidation by-products, because they should hopefully be less harmful than the parent compound(s). Actually, the environmental risk posed by a contaminant is not necessarily decreased by its degradation. Although the parent compound may not be persistent in the environment, the products formed may lengthen or even enhance the harmful effect of a contaminant, as described by several authors (e.g. [65]).

One simple way to evaluate this effect is by performing microtoxicity tests, which consist on testing the inhibition of some microorganisms. For instance, Fig. 14 shows that the acute toxicity to marine bacteria *V. fischeri* increased during the first 2 h of the catalytic tyrosol photo-degradation, which was attributed to the formation of phenolic by-products like 3,4-dihydroxyphenylethanol (hydroxytyrosol) [56]. However, as the reaction proceeded, the toxicity decreased due to the removal of both the original tyrosol and the by-products, as confirmed by the authors by HPLC analysis.

Other studies also addressed this issue, particularly when treating olive mill wastewaters and aiming the integration of the

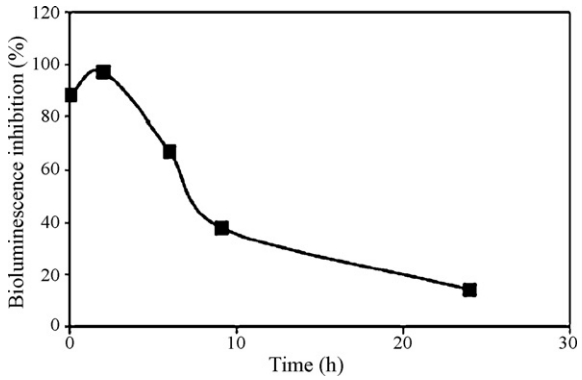


**Fig. 14.** Toxicity against *V. fischeri* during tyrosol degradation. [Tyrosol] = 500 ppm, $T = 25\,^{\circ}C$, $[H_2O_2] = 2 \times 10^{-2}$ M, pH 5, and $\lambda = 254$ nm [56]. Reprinted from Applied Catalysis B: Environmental, 74/1-2, W. Najjar, S. Azabou, S. Sayadi, A. Ghorbel, Catalytic wet peroxide photo-oxidation of phenolic olive oil mill wastewater contaminants: Part I. Reactivity of tyrosol over (Al–Fe)PILC, Copyright (2007), with permission from Elsevier.

photo-Fenton with a biological process [57]. In this study, the toxicity of a pre-treated model OMW was reduced by 74% and the subsequent biological treatment (using a methanogenic consortium) removed the remaining phenolic compounds by more than 70%, even with the most recalcitrant compounds tested (p-coumaric acid and tyrosol).

## 5. Mechanistic studies

Up to our knowledge, there are no studies available in the literature reporting the identification/quantification of intermediates and establishing reaction mechanisms during photo-Fenton heterogeneous processes based on PILCs. Although without carrying out such detailed studies, Feng et al., during degradation of either reactive red HE-3B [33] or Orange II [62] dyes, with a laponite based material (Fe-Lap-RD), have proposed the following rather simple mechanism:

$$Fe^{3+} \text{ on the surface of Fe-Lap-RD} + h\nu \rightarrow Fe^{2+} \text{ on the surface of Fe-Lap-RD} \quad (10)$$

$$Fe^{2+} \text{ on the surface of Fe-Lap-RD} + H_2O_2 \rightarrow Fe^{3+} \text{ on the surface of Fe-Lap-RD} + HO^{\bullet} + OH^{-} \quad (11)$$

$$\text{Fe-Lap-RD – dye} + HO^{\bullet} \rightarrow \text{Fe-Lap-RD—Reaction intermediates} \quad (12)$$

$$\text{Fe-Lap-RD – Reaction intermediates} + HO^{\bullet} \rightarrow CO_2 + H_2O \quad (13)$$

The reactions are thus initiated by the photo-reduction of $Fe^{3+}$ on the surface of Fe-Lap-RD to $Fe^{2+}$ under irradiation of UV light. Then, the $Fe^{2+}$ formed on the surface of the solid accelerates the decomposition of $H_2O_2$ in solution, generating highly oxidative HO radicals, while it is oxidized by $H_2O_2$ into $Fe^{3+}$ (Fenton's reaction). The generated $HO^{\bullet}$ species attack the dye molecules adsorbed on the surface of the clay, giving rise to reaction intermediates. Finally, the reaction intermediates are mineralized on the clay surface into $CO_2$ and $H_2O$ [33,62].

The role of the organics adsorption is still not clear, although some authors claim that strong adsorption of the organic reactant seems to be a necessary condition for the reaction to occur. Indeed, De León et al. argue that degradation is extremely poor for organic compounds exhibiting no significant chemisorption on the Fe-PILCs, even in the presence of UV radiation (photo-Fenton system) [11].

Another curious issue reported by these authors is the discoloration of methylene blue solutions in the absence of $H_2O_2$ [11]. In such conditions, they propose the formation of $HO^{\bullet}$ directly from photoactive Fe(III) hydroxycomplexes on the surface of Fe-PILC, as described in Eq. (4) for the homogeneous system. Re-oxidation of Fe(II) by oxygen has been suggested to take place according to the following equations:

$$Fe^{2+} + O_2 + H_2O \rightarrow Fe(OH)^{2+} + HO_2^{\bullet} \quad (14)$$

$$2HO_2^{\bullet} \rightarrow H_2O_2 + O_2 \quad (15)$$

Another interesting mechanism is the one proposed recently by Chen et al., who used visible light [63]. The mechanism is somewhat more elaborated than the ones described above, because they consider also direct photolysis of $H_2O_2$, excitation of the dye (reactive brilliant orange X-GN), dark Fenton, among other reactions as shown below:

$$H_2O_2 + \text{visible light} \rightarrow HO^{\bullet} + OH^{-} \quad (16)$$

$$\text{X–GN} + \text{visible light} \rightarrow \text{X–GN}* \quad (17)$$

$$\text{Fe(III)species} + \text{X–GN}* \rightarrow \text{Fe(II)species}(e^{-}) + \text{X–GN}^{+\bullet} \quad (18)$$

$$H_2O_2 + \text{Fe(II)species}(e^{-}) \rightarrow HO^{\bullet} + \text{Fe(III)species} \quad (19)$$

$$\text{Fe(III)species} + H_2O_2 \rightarrow \text{Fe(II)species} + HO_2^{\bullet} + H^{+} \quad (20)$$

$$\text{Fe(II)species} + H_2O_2 \rightarrow \text{Fe(III)species} + HO^{\bullet} + OH^{-} \quad (21)$$

$$\text{X–GN} * + Fe^{3+} \rightarrow Fe^{2+} + \text{X–GN}^{+\bullet} \quad (22)$$

$$Fe^{2+} + H_2O_2 \rightarrow Fe^{3+} + OH^{-} + HO^{\bullet} \quad (23)$$

$$HO^{\bullet} + \text{X–GN} \rightarrow \text{X–GN degraded products} \quad (24)$$

$$HO^{\bullet} + \text{X–GN}^{+\bullet} \rightarrow \text{X–GN degraded products} \quad (25)$$

## 6. Modeling

The development of phenomenological models of chemical processes is of extreme importance from both the fundamental and applied points of view. On one hand it allows, after experimental validation, to have a better insight about the involved phenomena, the process itself, etc. On the other hand, it provides a tool for the design and optimization, in particular for the design of better and more efficient photo-reactors. But for that, it is mandatory to firstly determine the rate equations via kinetic studies. In this section, we will describe the main modeling works reported in the literature in the context of this review.

### 6.1. Lumped models

Because the reaction networks involved in wastewater treatment through AOPs are rather complex, several authors have adopted the methodology of lumped models. An interesting example is provided in the kinetic study reported recently by Iurascu et al. during the photo-Fenton degradation of phenol [54]. Due to the complexity associated with the identification and quantification of the numerous intermediates, a General Lumped Kinetic Model (GLKM) was proposed:

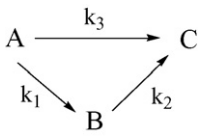


(26)

where A stands for phenol, B for all the intermediates, and C for the final oxidation products ($CO_2$, $H_2O$). In such a model, $k_1$, $k_2$, $k_3$

are apparent first-order rate constants. Although not remarked by the authors, it should be highlighted that because we are dealing with a heterogeneous process, the units reported for the rate constants (time$^{-1}$) results from the fact that they include the catalyst concentration.

The mass balances for the involved species are as follows:

$$\frac{dC_A}{dt} = -(k_1 + k_3)C_A \quad (27)$$

$$\frac{dC_B}{dt} = k_1 C_A - k_2 C_B \quad (28)$$

Based on the known initial concentrations ($C_{A_0}$ and 0 for A and B, respectively), the following solutions result:

$$C_A = C_{A_0}\, e^{-(k_1+k_3)t} \quad (29)$$

$$C_B = \frac{k_1 C_{A_0}}{k_2 - k_1}(e^{-k_1 t} - e^{-k_2 t}) \quad (30)$$

Taking into account that $C_A + C_B = TOC$ and, as stated by the authors, that $k_3$ should be much smaller than $k_1$ or $k_2$ (because a direct conversion of phenol into $CO_2$ and water is not expected), the GLKM becomes a consecutive reaction model, wherein:

$$\frac{C_A + C_B}{C_{A_0}} = \frac{TOC}{TOC_0} = \frac{k_1}{k_1 - k_2}\, e^{-k_2 t} - \frac{k_2}{k_1 - k_2}\, e^{-k_1 t} \quad (31)$$

This equation, in the linearized form, was then fitted to experimental TOC data along time, from which $k_1$ and $k_2$ were estimated with significant regression factors for all Fe-laponite samples tested. For all the solids, $k_1$ is between two and three times lower than $k_2$ (in the range 0.0047–0.0080 and 0.0096–0.0197 min$^{-1}$, respectively), which means that the reaction phenol → intermediates is much slower than the reaction intermediates → $CO_2$ + $H_2O$ [54].

### 6.2. Langmuir-Hinshelwood rate equations

Different kinetic strategies can be found in the literature for the interpretation and modeling of photo-Fenton-like oxidation processes using PILCs, in particular using well-known Langmuir-Hinshelwood (LH) formulations. It is worth mentioning, for instance, the kinetics of the tyrosol conversion by wet peroxide photo-oxidation (using an Al–Fe montmorillonite), reported by Najjar et al. [56]. Based on their experimental results, a model was proposed in which two types of active sites were hypothesized to exist on the catalyst surface: on the first ones the competitive adsorption of tyrosol and the intermediate products of degradation occurred while on the second ones hydrogen peroxide was adsorbed. Assuming that the activation of the adsorbed organic molecule by OH radicals is the rate determining step, these authors concluded that the photodegradation rate can be expressed by a LH kinetics as follows:

$$r_{tyrosol} = k\theta_{H_2O_2}\theta_{tyrosol} \quad (32)$$

where,

$$\theta_{H_2O_2} = \frac{K_{H_2O_2} C_{H_2O_2}}{1 + K_{H_2O_2} C_{H_2O_2}} \quad (33)$$

$$\theta_{tyrosol} = \frac{K_{tyrosol} C_{tyrosol}}{1 + K_{tyrosol} C_{tyrosol} + \sum_i K_i C_i} \quad (34)$$

In this scheme, $\theta_{H_2O_2}$ and $\theta_{tyrosol}$ are the fractions of the sites covered by $H_2O_2$ and tyrosol, respectively, subscript $i$ stands for reaction intermediates, and $K$ symbols refer to equilibrium adsorption constants. Considering that $K_{tyrosol}C_{tyrosol} + \sum_i K_i C_i = K_{tyrosol}C_{tyrosol,o}$, where $C_{tyrosol,o}$ represents the initial concentration of tyrosol, and after introducing the dependence of the apparent rate constant with the temperature, the following LH equation was obtained:

$$r_{tyrosol} = k_o\, e^{\left(-\frac{E_a}{RT}\right)} \times \frac{K_{tyrosol} C_{tyrosol} K_{H_2O_2} C_{H_2O_2}}{(1 + K_{tyrosol} C_{tyrosol,o})(1 + K_{H_2O_2} C_{H_2O_2})} \quad (35)$$

It is quite important to experimentally validate the models proposed. The authors simply state that in the conditions employed, the established kinetic model is in line with the experimental data [56].

### 6.3. Apparent first-order rate equations

Apparent rate equations have been often adopted in modeling works, in most cases first-order kinetic equations with respect to the parent compound. These equations are not phenomenological, but we decided to include them anyway because they can still be very useful in reactor design. We call them "apparent" because several processes can contribute to the overall conversion of the parent compound, even though the extent and contribution of each one is not known in detail (e.g., adsorption of the species on the PILC surface, heterogeneous or homogeneous oxidation, oxidation promoted by radicals coming from direct photolysis of $H_2O_2$ or direct photolysis of the parent compound/intermediates, etc.).

One example reported in the literature is the photo-Fenton degradation of an azo-dye, acid black 1 (AB1), over a modified laponite clay-based Fe nanocomposite (Fe-Lap-RD) by Sum et al. [31]. The authors proposed Eq. (36) for the kinetics of the photocatalytic discoloration, which allows computing the corresponding half-life value ($t_{1/2}$) through Eq. (37):

$$r = -\frac{dC}{dt} = kC \quad (36)$$

$$t_{1/2} = \frac{0.693}{k} \quad (37)$$

Here, $k$ is the apparent pseudo first-order rate constant, for the reasons state above, $C$ is the concentration of the parent compound and $t$ the time. As usual, the rate constant is obtained from the slope of a straight line by plotting the value of $\ln(C/C_o)$ along time, although only the values of the first 15 min have been used in this work [31]. By applying the Arrhenius law (Eq. (38)), the apparent activation energy was then computed (24.71 kJ/mol).

$$k = k_o\, e^{-E_a/RT} \quad (38)$$

In Eq. (38), $k_o$ is the pre-exponential factor (min$^{-1}$), $E_a$ is the apparent activation energy (J/mol), $T$ is the reaction temperature (K) and $R$ is the ideal gas constant.

A similar approach has been used by other authors, particularly for analyzing the effect of some operating conditions (e.g. pH) in the pseudo first-order rate constants. For instance, Feng et al. obtained maximum apparent kinetic constants at an initial pH of 3.0 for both bentonite- and laponite-based catalysts during Orange II discoloration (0.193 and 0.172 min$^{-1}$, respectively) [61]. Bobu and co-workers came to the same conclusion when performing experiments at different pH values during photo-Fenton mineralization of ciprofloxacin with a pillared laponite containing iron [65].

## 7. Conclusions and future perspectives

To avoid the disadvantages associated to the homogeneous photo-Fenton/photo-Fenton-like processes, i.e. transition metal catalyst loss or implementation of technologies to recover it after wastewater treatment, heterogeneous materials have been developed to support the metal (particularly iron) active phases. This review is focused on the use of pillared clays for such purposes, aiming either the degradation of model compounds or real wastewaters treatment. PILCs deserved the attention of numerous researchers

for these (and other) applications, particularly due to their characteristics, abundance and low cost, as well as to the fact of being tunable in terms of properties, according to the final application envisaged.

To better understand the involved phenomena and more easily optimize the operating conditions, an exhaustive analysis was performed focused on the analysis of each factor in the overall performance. This included the analysis of the effect of parameters like pH, temperature, reactants and pollutants doses, type and power of light, type of catalyst, etc. Nevertheless, from the applied point of view one should also take into account other issues that have also been discussed in detail. These include, for instance, catalyst stability. Besides, for industrial application of these AOPs, the use of continuous-flow reactors should be considered, e.g. of the thin-film type, as well as the possibility of using visible radiation, thus making use of a wider range of the solar spectrum. Another important technological issue to consider in practice is the mode of the oxidant (hydrogen peroxide) addition, as it represents one important operating cost. Thus, its efficient use should be carefully optimized.

The use of integrated processes that combine AOPs, as preliminary steps, with biological treatments of wastewaters containing refractory compounds is effective to achieve complete degradation of pollutants and seems to be attractive, from an economical point of view. Nevertheless, the opposite assembly could be also considered, where the AOP would be used as a final polishing stage. To define the better strategy it is mandatory to evaluate also the final impact of the integrated process, and thus the toxicity of the intermediate and final products should be accounted for. This could in principle be coupled with detailed analytical techniques to identify the compounds produced, allowing at the same time the establishment of better and more realistic mechanisms. As a consequence, more elaborated models could be developed, which could in turn provide the opportunity to scale-up and design better and more efficient photo-reactors.

## Acknowledgements

M.A. Vicente thanks financial support from Spanish Science and Innovation Ministry and ERDF Funds (MAT2007-66439-C02).

## References

[1] V.J. Inglezakis, S.G. Poulopoulos, Adsorption, Ion Exchange and Catalysis: Design of Operations and Environmental Applications, Elsevier Science, 2006.
[2] R. Andreozzi, V. Caprio, A. Insola, R. Marotta, Catal. Today 53 (1999) 51.
[3] I. Casero, D. Sicilia, S. Rubio, D. Perez-Bendito, Water Res. 31 (1997) 1985.
[4] O. Legrini, E. Oliveros, A.M. Braun, Chem. Rev. 93 (1993) 671.
[5] W.H. Glaze, J.W. Kang, Ind. Eng. Chem. Res. 28 (1989) 1573.
[6] W.R. Haag, C.C.D. Yao, Environ. Sci. Technol. 26 (1992) 1005.
[7] G.R. Peyton, F.R. Huang, J.L. Burleson, W.H. Glaze, Environ. Sci. Technol. 16 (1982) 454.
[8] L.F. Liotta, M. Gruttadauria, G. Di Carlo, G. Perrini, V. Librando, J. Hazard Mater. 162 (2009) 588.
[9] R. Andreozzi, R. Marotta, Water Res. 38 (2004) 1225.
[10] G. Mailhot, L. Hykrdová, J. Jirkovský, K. Lemr, G. Grabner, M. Bolte, Appl. Catal. B: Environ. 50 (2004) 25.
[11] M.A. De León, J. Castiglioni, J. Bussi, M. Sergio, Catal. Today 133 (2008) 600.
[12] J. Feng, X. Hu, P.L. Yue, S. Qiao, Sep. Purif. Tech. 67 (2009) 213.
[13] J. Feng, X. Hu, P.L. Yue, H.Y. Zhu, G.Q. Lu, Ind. Eng. Chem. Res. 42 (2003) 2058.
[14] F. Martínez, G. Calleja, J.A. Melero, R. Molina, Appl. Catal. B: Environ. 60 (2005) 181.
[15] M. Noorjahan, D.V. Durga Kumari, M. Subrahmanyam, L. Panda, Appl. Catal. B: Environ. 57 (2005) 291.
[16] T.J. Pinnavaia, Science 220 (1983) 365.
[17] A. Gil, L.M. Gandía, M.A. Vicente, Catal. Rev. Sci. Eng. 42 (2000) 145.
[18] A. Gil, S.A. Korili, M.A. Vicente, Catal. Rev. Sci. Eng. 50 (2008) 153.
[19] H.J.H. Fenton, J. Chem. Soc. 65 (1894) 899.
[20] F. Haber, J. Weiss, Proc. R. Soc. Lond. 147 (1934) 332.
[21] H. Gallard, J. De Laat, Water Res. 34 (2000) 3107.
[22] M. Pera-Titus, V. García-Molina, M.A. Baños, J. Giménez, S. Espulgas, Appl. Catal. B: Environ. 47 (2004) 219.
[23] C. Walling, Acc. Chem. Res. 8 (1975) 125.
[24] M. Kitis, C.D. Adams, G.T. Daigger, Water Res. 33 (1999) 2561.
[25] J. Yoon, Y. Lee, S. Kim, Water Sci. Technol. 44 (2001) 15.
[26] M.C. Lu, C.J. Lin, C.H. Liao, W.P. Ting, R.Y. Huang, Water Sci. Technol. 44 (2001) 327.
[27] E.G. Garrido-Ramírez, B.K.G. Theng, M.L. Mora, Appl. Clay Sci. 47 (2010) 182.
[28] J. Herney-Ramírez, L.M. Madeira, in: A. Gil, S.A. Korili, R. Trujillano, M.A. Vicente (Eds.), Pillared Clays and Related Catalysts, Springer, 2010.
[29] S. Malato, J. Blanco, A. Vidal, C. Richter, Appl. Catal. B: Environ. 37 (2002) 1.
[30] P.R. Gogate, A.B. Pandit, Adv. Environ. Res. 8 (2004) 553.
[31] O.S.N. Sum, J. Feng, X. Hu, P.L. Yue, Top. Catal. 33 (2005) 233.
[32] A.C.-K. Yip, F.L.-Y. Lam, X. Hu, Ind. Eng. Chem. Res. 44 (2005) 7983.
[33] J. Feng, X. Hu, P.L. Yue, H.Y. Zhu, G.Q. Lu, Water Res. 37 (2003) 3776.
[34] G. Centi, S. Perathoner, T. Torre, M.G. Verduna, Catal. Today 55 (2000) 61.
[35] K.C. Gupta, A.K. Sutar, Polym. Adv. Technol. 19 (2008) 186.
[36] J.H. Ramírez, C.A. Costa, L.M. Madeira, G. Mata, M.A. Vicente, M.L. Rojas-Cervantes, A.J. López-Peinado, R.M. Martín-Aranda, Appl. Catal. B: Environ. 71 (2007) 44.
[37] M.N. Timofeeva, M.S. Mel'gunov, O.A. Kholdeeva, M.E. Malyshev, A.N. Shmakov, V.B. Fenelonov, Appl. Catal. B: Environ. 75 (2007) 290.
[38] E. Guélou, J.M. Tatibouët, J. Barrault, in: A. Gil, S.A. Korili, R. Trujillano, M.A. Vicente (Eds.), Pillared Clays and Related Catalysts, Springer, 2010.
[39] M.N. Timofeeva, S.Ts. Khankhasaeva, Y.A. Chesalov, S.V. Tsybulya, V.N. Panchenko, E.Ts. Dashinamzhilova, Appl. Catal. B: Environ. 88 (2009) 127.
[40] W.Y. Lee, B.J. Tatarchuk, Hyperfine Interact. 41 (1988) 661.
[41] W.Y. Lee, R.H. Raythatha, B.J. Tatarchuk, J. Catal. 115 (1989) 159.
[42] F. Bergaya, N. Hassoun, J. Barrault, L. Gatineau, Clay Miner. 28 (1993) 109.
[43] T. Bakas, A. Moukarika, V. Papaefthymiou, A. Ladavos, Clays Clay Miner. 42 (1994) 634.
[44] I. Pálinkó, K. Lázár, I. Kiricsi, J. Mol. Struct. 410–411 (1997) 547.
[45] I. Pálinkó, A. Molnár, J.B. Nagy, J.-C. Bertrand, K. Lázár, J. Valyon, I. Kiricsi, J. Chem. Soc. Faraday Trans. 93 (1997) 1591.
[46] W. O'Neil Parker Jr., R. Millini, I. Kiricsi, Inorg. Chem. 36 (1997) 571.
[47] T. Mandalia, M. Crespin, D. Messad, F. Bergaya, J. Chem. Soc. Chem. Comm. 19 (1998) 2111.
[48] E. Guélou, J. Barrault, J. Fournier, J.-M. Tatibouët, Appl. Catal. B: Environ. 44 (2003) 1.
[49] C. Belver, M.A. Vicente, A. Martínez-Arias, M. Fernández-García, Appl. Catal. B: Environ. 50 (2004) 227.
[50] J. Carriazo, E. Guélou, J. Barrault, J.-M. Tatibouët, R. Molina, S. Moreno, Water Res. 39 (2005) 3891.
[51] M.N. Timofeeva, S.Ts. Khankhasaeva, S.V. Badmaeva, A.L. Chuvilin, E.B. Burgina, A.B. Ayupov, V.N. Panchenko, A.V. Kulikova, Appl. Catal. B: Environ. 59 (2005) 243.
[52] M.N. Timofeeva, S.Ts. Khankhasaeva, E.P. Talsi, V.N. Panchenko, A.V. Golovin, E.Ts. Dashinamzhilova, S.V. Tsybulya, Appl. Catal. B: Environ. 90 (2009) 618.
[53] J.G. Carriazo, E. Guelou, J. Barrault, J.M. Tatibouet, S. Moreno, Appl. Clay Sci. 22 (2003) 303.
[54] B. Iurascu, I. Siminiceanu, D. Vione, M.A. Vicente, A. Gil, Water Res. 43 (2009) 1313.
[55] E.E. Kiss, M.M. Lazic, G.C. Boskovic, React. Kinet. Catal. Lett. 83 (2004) 221.
[56] W. Najjar, S. Azabou, S. Sayadi, A. Ghorbel, Appl. Catal. B: Environ. 74 (2007) 11.
[57] S. Azabou, W. Najjar, A. Gargoubi, A. Ghorbel, S. Sayadi, Appl. Catal. B: Environ. 77 (2007) 166.
[58] R.B. Achma, A. Ghorbel, S. Sayadi, A. Dafinov, F. Medina, J. Phys. Chem. Solids 69 (2008) 1116.
[59] O.S.N. Sum, J. Feng, X. Hu, P.L. Yue, Chem. Eng. Sci. 59 (2004) 5269.
[60] J. Feng, R.S.K. Wong, X. Hu, P.L. Yue, Catal. Today 98 (2004) 441.
[61] J. Feng, X. Hu, P.L. Yue, Water Res. 40 (2006) 641.
[62] J. Feng, X. Hu, P.L. Yue, H.Y. Zhu, G.Q. Lu, Chem. Eng. Sci. 58 (2003) 679.
[63] Q. Chen, P. Wu, Y. Li, N. Zhu, Z. Dang, J. Hazard. Mater. 168 (2009) 901.
[64] M.M. Bobu, I. Siminiceanu, E. Lundanes, Rev. Chim. 58 (2007) 988.
[65] M. Bobu, A. Yediler, I. Siminiceanu, S. Schulte-Hostede, Appl. Catal. B: Environ. 83 (2008) 15.
[66] P.A. Carneiro, R.F. Pupo Nogueira, M.V.B. Zanoni, Dyes Pigments 74 (2007) 127.
[67] M.F. Monaco, M.F. Asthon, C.S. Weller, Weed Science: Principles and Practices, Wiley, New York, 2002.
[68] A.B. Caracciolo, G. Giuliano, P. Grenni, L. Guzzella, F. Pozzoni, P. Bottoni, L. Fava, A. Crobe, M. Orrù, E. Funari, Environ. Pollut. 134 (2005) 525.
[69] E.M. Golet, I. Xifra, H. Siegrist, A.C. Alder, W. Giger, Environ. Sci. Technol. 37 (2003) 3243.
[70] E.M. Golet, A.C. Alder, W. Giger, Environ. Sci. Technol. 36 (2000) 3645.
[71] V.A. Nadtochenko, J. Kiwi, Inorg. Chem. 37 (1999) 5233.
[72] J. Feng, X. Hu, P.L. Yue, Water Res. 39 (2005) 89.
[73] P.L. Huston, J.J. Pignatello, Water Res. 33 (1999) 1238.
[74] X.-Y. Li, Y.-H. Cui, Y.-J. Feng, Z.-M. Xie, J.-D. Gu, Water Res. 39 (2005) 1972.
[75] L. Kong, J.L. Ferry, Environ. Sci. Technol. 37 (2003) 4894.
[76] M. Cheng, W. Ma, C. Chen, J. Yao, J. Zhao, Appl. Catal. B: Environ. 65 (2006) 217.

[77] Y.X. Liu, X. Zhang, L. Guo, F. Wu, N.S. Deng, Ind. Eng. Chem. Res. 47 (2008) 7141.
[78] Q. Chen, P. Wu, Z. Dang, N. Zhu, P. Li, J. Wu, X. Wang, Sep. Purif. Technol. 71 (2010) 315.
[79] C.D. Stalikas, L. Lunar, S. Rubio, D. Peĭrez-Bendito, Water Res. 35 (2001) 3845.
[80] G. Calleja, J.A. Melero, F. Martínez, R. Molina, Water Res. 39 (2005) 1741.
[81] Y.F. Wang, W.H. Ma, C.C. Chen, X.F. Hu, J.C. Zhao, J.C. Yu, Appl. Catal. B: Environ. 75 (2007) 256.